ALGORITHMS FOR BETTER FLUX ESTIMATION

AND

MODEL PREDICTIVE CONTROL OF INDUCTION MOTOR

DISSERTATION
SUBMITTED IN PARTIAL FULFILLMENT OF THE REQUIREMENTS
FOR THE AWARD OF THE DEGREE
OF

MASTER OF TECHNOLOGY
IN
CONTROL AND INSTRUMENTATION

Submitted by:

Apurva Pratap Singh

Roll No. 2K15/C&I/06

Under the supervision of

Prof. Narendra Kumar (II)

DEPARTMENT OF ELECTRICAL ENGINEERING
DELHI TECHNOLOGICAL UNIVERSITY
(Formerly Delhi College of Engineering)
Bawana Road, Delhi-110042

2017

DEPARTMENT OF ELECTRICAL ENGINEERING

DELHI TECHNOLOGICAL UNIVERSITY

(Formerly Delhi College of Engineering)

Bawana Road, Delhi-110042

CERTIFICATE

I, Apurva Pratap Singh, Roll No. 2K15/C&I/06 student of M.Tech. control and instrumentation (C&I), hereby declare that the dissertation/project titled **"Algorithms for Better Flux Estimation and Model Predictive Control of Induction Motor"** under the supervision of Prof. Narendra Kumar(II) of Electrical Engineering Department, Delhi Technological University, Delhi in partial fulfillment of the requirement for the award of the degree of Master of Technology has not been submitted elsewhere for the award of any Degree.

.

Place: Delhi

Date: 13/07/2017

(APURVA PRATAP SINGH)

Prof. NARENDRA KUMAR (II)

(SUPERVISOR)

Professor

Department of Electrical Engineering

Delhi Technological University

ACKNOWLEDGEMENT

I am highly grateful to the Department of Electrical Engineering, Delhi Technological University (DTU) for providing this opportunity to carry out the project work.

The constant guidance and encouragement received from my supervisor Prof. Narendra Kumar (II) of Department of Electrical Engineering, DTU, has been of great help in carrying my present work and is acknowledged with reverential thanks.

I would like to thank Mr. Ambrish Devanshu (PhD scholar) for his guidance and his continuous support throughout this course work.

I would like to express a deep sense of gratitude and thanks to PROF. MADHUSHUDAN SINGH for providing the laboratory and other facilities to carryout the project work. Again, the help rendered by Prof. Narendra Kumar (II) , for the literature, and for experimentation is greatly acknowledged.

Finally, I would like to expresses gratitude to other faculty members of Electrical Engineering Department, DTU for their intellectual support throughout the course of this work.

APURVA PRATAP SINGH
2K15/C&I/06
M. Tech. (Control and Instrumentation)
Delhi Technological University

ABSTRACT

In this project the analysis of flux estimation algorithms is carried out and the concept of Model Predictive Current Control is implemented on Induction Motor. In any controlling scheme the estimation part is the most important as if the estimation is not correct no matter how good the controlling scheme the controlling cannot be better, in Induction Motor Vector Control the estimation of flux is done by integrating back emf, with pure integration there exist problems such as saturation and initial value problems which dominate the results when the machine is operating at low frequencies, to eliminate these problems various algorithms are implemented on the simulink MATLAB and their results are discussed. The estimated flux must follow the measured flux, the more the error between them the poor is the controlling.

Model Predictive Control is a controlling algorithm which was used for process control systems, but with time because of its constraint handling technique it is implemented on drives also. A simple Predictive Current Control algorithm is implemented on the Induction Motor Drive with Direct Vector Control. The hysteresis control is replaced by the model predictive algorithm. the results are obtained with different running conditions of Induction Motor.

CONTENTS

LIST OF FIGURES

LIST OF TABLES

ABBREVIATIONS

DTC	Direct Torque Control
FOC	Field Oriented Control
MPC	Model Predictive Control
LPF	Low Pass Filter
IM	Induction Motor
PI	Proportional-Integral
AC	Alternating Current
DC	Direct current

LIST OF SYMBOLS

E_b	Back EMF of Induction Motor
T_d	Developed Torque
T_l	Load Torque
ω_m	Angular frequency of Induction Motor
ω_{slip}	Slip angular frequency
I_a	Armature Current
I_{abc}	Three phase current vector
$I_{\alpha\beta\gamma}$	Two phase stationary reference frame current vector
I_{dq0}	Two phase rotating reference frame current vector
R_s	Stator Resistance
R_r	Rotor Resistance
L_r	Rotor self Inductance
L_s	Stator self Inductance
L_m	Mutual Inductance of Induction Motor
I_q	Q axis current(Rotating frame of reference)
I_d	D axis current(Rotating frame of reference)
I_α	α axis current(Stationary frame of reference)
I_β	β axis current(Stationary frame of reference)
V_q	Q axis voltage(Rotating frame of reference)
V_d	D axis voltage(Rotating frame of reference)
V_α	α axis voltage(Stationary frame of reference)
V_β	β axis voltage(Stationary frame of reference)
Z_{comp}	Compensated feedback
λ	Lambda(tuning parameter)
Ψ_s	Total stator flux
Ψ_r	Rotor flux
Ψ_m	Magnetizing component of flux
i(k+1)	Predicted current
i*(k+1)	Predicted reference current
g	Objective function
i(k)	Present value of current
v(k)	Voltage vector
Ts	Sampling time

CHAPTER 1

INTRODUCTION

1.1. INTRODUCTION

Induction Motor drives are used in almost all the industrial applications because of their rugged and robust performance, also the performance of Induction Motor is very promising in high speed applications. If we compare Induction Motor and DC motor, then the main advantage that DC motor have over Induction Motor is its continuously controlling of speed. It can be clearly seen from these equations 1.1(a) and 1.1(b) that the torque and speed are decoupled from each other, in other words we can say that by effecting the torque, speed will not be get effected and vice versa.

$$E_b = \frac{P.\Psi.Z.\omega_m}{2.\pi.A} \qquad (1.1(a))$$

$$T_d = \frac{P.\Psi.Z.I_a}{2.\pi.A} \qquad (1.1(b))$$

where P is number of poles, Z is total number of conductors, E_b is the back emf of motor, T_d is the developed torque, ω_m is the angular mechanical speed, I_a is the armature current, A is the number of parallel paths and Ψ is the flux of motor.

In DC machines mmf axis is established at 90˚ electrical to the main field axis. The electromagnetic torque is proportional to the product of field flux and armature current. Field flux is proportional to the field current and is unaffected by the armature current because of orthogonal orientation between armature mmf and field mmf. Therefore in a separately excited DC machine, with a constant value of field flux the torque is directly proportional to the armature current. Hence direct control of armature current gives direct control of torque

and fast response. In Induction Motor the flux and torque components are mutually coupled, so the controlling of Induction Motor as compared to DC motor is not effective. But DC motor is not economical it has the additional cost of maintenance of brushes, brush holders, commutators etc, and the initial cost of DC motor is also more. So, a substitute is needed which is economical as well as have better controlling in transient and steady state. As discussed Induction Motor are robust and rugged and have almost no maintenance cost, so it can be used in place of the DC motor if we can decouple the flux and torque component of Induction Motor then the controlling similar to the DC motor controlling can be achieved[45].

Induction Motor controlling can be classified broadly into two parts:

a) Scalar control of Induction Motor

b) Vector control of Induction Motor

Above control schemes can be further divided, Figure 1 shows the various Vector Control Schemes for controlling Induction Motor.

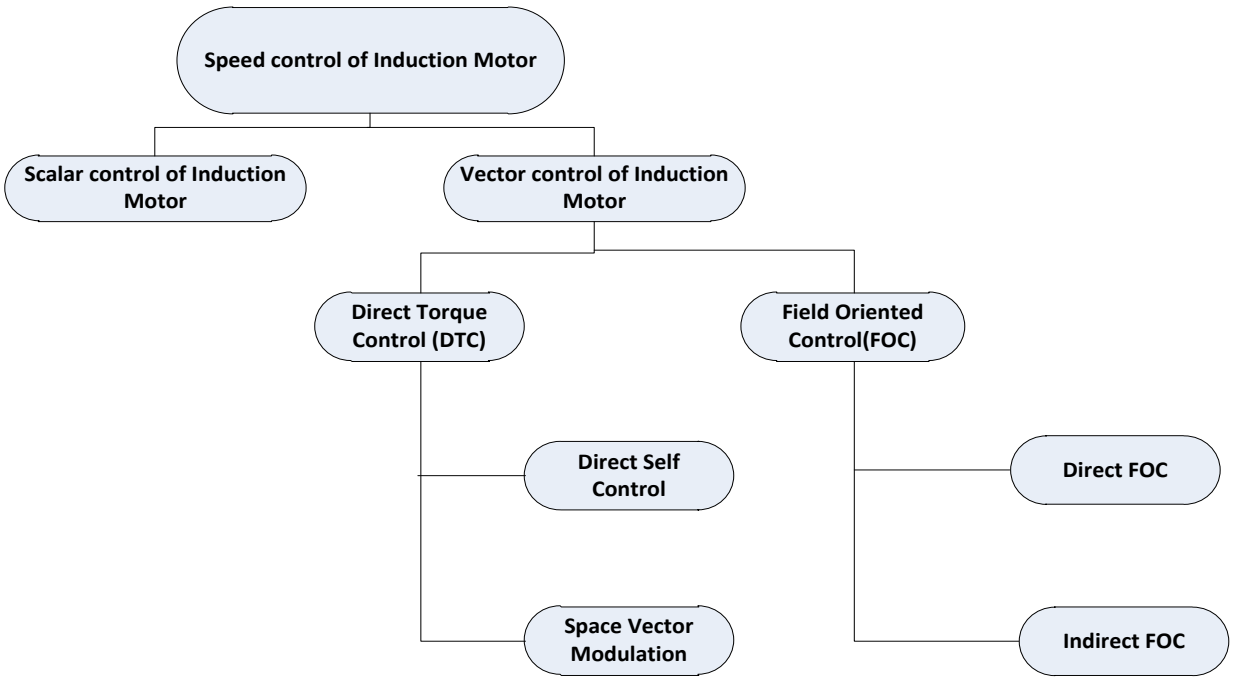

Fig.1. Classification of vector control methods used for speed control of Induction Motor

1.2. SCALAR CONTROL OF INDUCTION MOTOR

Now, there are various methods for scalar control of Induction Motor[34].

1) Pole changing method
2) Variable supply voltage control
3) Rotor resistance control
4) V/f control etc

1.2.1 Pole changing method

Speed control of cage type Induction Motors can be done by this method, because in cage type IM the number of poles is equal to the stator winding poles, so by this concept we can change the number of poles which in turn can control the speed of Induction Motor.

1.2.2. Variable supply voltage control

By varying the voltage the speed can be controlled. We know that the torque of IM is directly proportional to square of the voltage, so until the required torque is not achieved the voltage is varied. This method is used where the load torque reduce with speed for example in fan loads. This method can be used for speed control only for below synchronous speeds, because if the voltage is increased then the insulation may breakdown.

1.2.3. Rotor resistance control

This method is used to control wound rotor type Induction Motor. A variable resistance can be connected through slip rings to the rotor circuit of Induction Motor. Now, we know that the maximum torque is independent of the rotor resistance, but the slip at which the maximum torque occurs depend upon the resistance. As the value of resistance increases,

larger will be the value of slip at which maximum torque occurs. Drawback of this method is due to the additional resistive losses.

1.2.4. V/f speed control

As we know that the synchronous speed is directly proportional to supplied frequency and also induced emf is directly proportional to supplied frequency. So, if supply frequency is changed, induced emf is also changed to maintain the same air gap flux. This method is efficient, but has a limitation as for this control variable supply frequency is needed i.e. Voltage source Inverter, Current source Inverter, Cycloconverter.

1.3. VECTOR CONTROL OF INDUCTION MOTOR

The method vector control of Induction Motor was initially developed by Blaschke. In vector control two quadrature components of three phase currents are synthesized, one of which is responsible for flux component which in turn effect the speed and the second component is responsible for the torque[16,24].

The methods from which the three phase quantities are transformed into two phase quadrature quantities are:

1) Clarke Transform
2) Park Transform

1.3.1. Clarke Transform

Clarke transformation is shown in Figure 2. It is used to transform the three phase quantities into stationary two phase quantities which are orthogonal to each other. Clarke transformation is given by following equation 1.2.

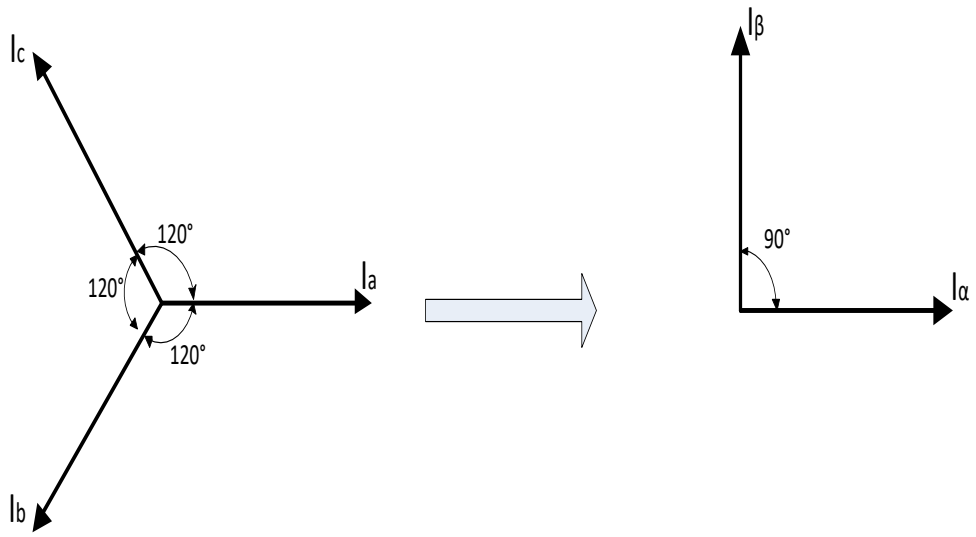

Fig.2. Clarke Transformation

$$I_{\alpha\beta\gamma} = \frac{2}{3}\begin{bmatrix} 1 & -\frac{1}{2} & -\frac{1}{2} \\ 0 & \frac{\sqrt{3}}{2} & -\frac{\sqrt{3}}{2} \\ \frac{1}{2} & \frac{1}{2} & \frac{1}{2} \end{bmatrix} . I_{abc} \qquad (1.2)$$

where I_a I_b I_c are three phase quantities and I_α I_β I_γ are transformed quantities and I_γ is zero as vector sum of three phase quantities displaced equally and of same magnitude is zero, so I_α and I_β are given by equation 1.3 and 1.4.

$$I_\alpha = \frac{2}{3}\left(I_a - \frac{1}{2}I_b - \frac{1}{2}I_c\right) \qquad (1.3)$$

$$I_\beta = \frac{1}{\sqrt{3}}(I_b - I_c) \qquad (1.4)$$

Also inverse Clarke transformation is used to transform the stationary two phase orthogonal components to three phase balanced components which is given by equation 1.5

$$I_{abc} = \begin{bmatrix} 1 & 0 & 1 \\ -\frac{1}{2} & \frac{\sqrt{3}}{2} & 1 \\ -\frac{1}{2} & -\frac{\sqrt{3}}{2} & 1 \end{bmatrix} . I_{\alpha\beta\gamma} \quad (1.5)$$

1.3.2. Park Transform

By Clarke transformation the 3 phase quantities are changed to stationary 2 phase quantities. Park transformation is used to transform the stationary frame reference to rotating frame reference and it is given by equation 1.6.

$$I_{dq} = \begin{bmatrix} \cos\theta & \sin\theta \\ -\sin\theta & \cos\theta \end{bmatrix} . I_{\alpha\beta} \quad (1.6)$$

where I_{dq} is the rotating reference frame quantities, $I_{\alpha\beta}$ are the stationary reference frame quantities and θ is the rotor angle that has to be known for calculating the park transformation matrix. Figure 3 shows the geometrical interpretation of park transformation.

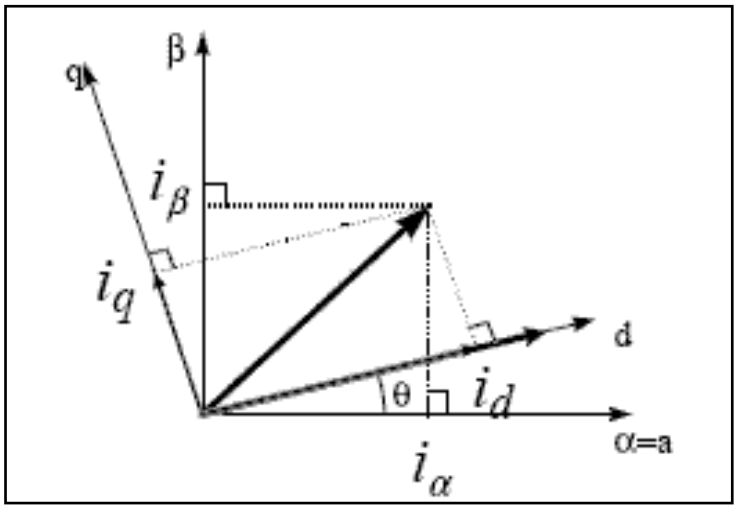

Fig.3. Park Transformation

The inverse park transformation is given by equation 1.7

$$I_{\alpha\beta} = \begin{bmatrix} \cos\theta & -\sin\theta \\ \sin\theta & \cos\theta \end{bmatrix} . I_{dq} \tag{1.7}$$

1.4. DIRECT TORQUE CONTROL SCHEME

In Direct Torque Control the flux and torque are estimated. The flux is estimated by integrating back emf, torque is then estimated by cross product of flux and stator quadrature currents. These estimated values are then compared to the preset reference values and if the deviation is high then the switching of power electronic device is done such that these values are brought back to their references. The reference values of torque and flux are obtained by reference speed. Reference speed and measured speed are compared and then with a PI regulator reference torque is obtained. Also the reference value of flux can be calculated through flux table. Figure 4 shows block diagram of Direct Torque Control scheme[17,47,9].

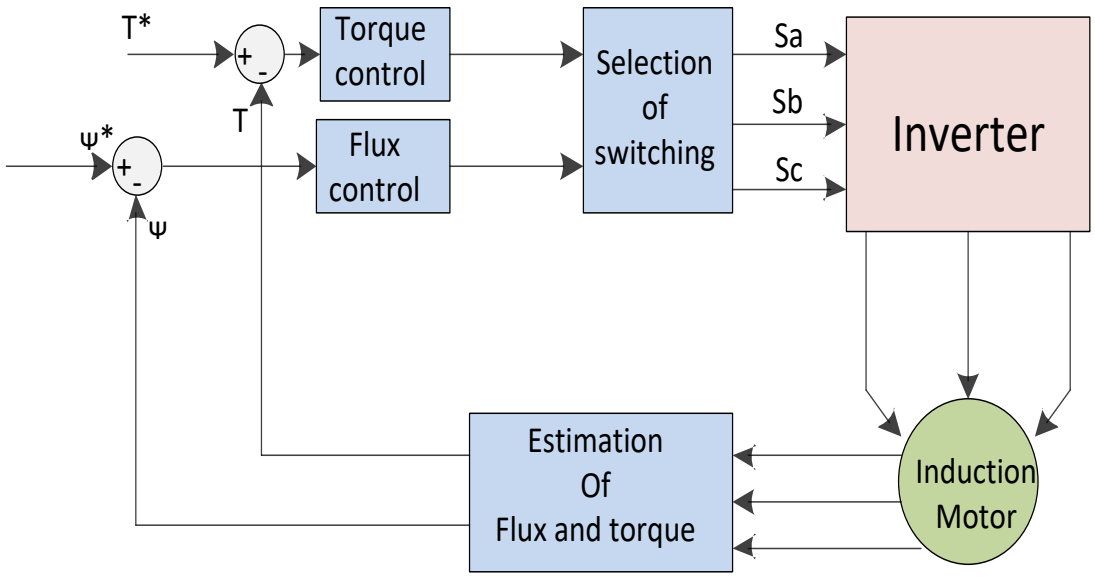

Fig.4. Block diagram for Direct Torque Control scheme

In Figure 4 Sa, Sb and Sc are showing the switching instants. As we know that a 3 phase inverter has three arms and six switches. Now for controlling the speed of Induction Motors different switching patterns are obtained. Three switches from different arms get ON and the remaining three gets OFF, and according to switching a voltage vector appears on the terminals of the 3 phase Induction Motor, which effects the performance of Induction Motor. Figure 5 shows the different switching states. Here the vectors showing 0 and 1 show the states of switching state Sa, Sb and Sc, which is explained by equation 1.8(a), 1.8(b) and 1.8(c).

$$Sa = \begin{Bmatrix} 1\ if\ S1\ is\ ON\ and\ S4\ is\ OFF \\ 0\ if\ S1\ is\ OFF\ and\ S4\ is\ ON \end{Bmatrix} \quad (1.8(a))$$

$$Sb = \begin{Bmatrix} 1\ if\ S2\ is\ ON\ and\ S5\ is\ OFF \\ 0\ if\ S2\ is\ OFF\ and\ S5\ is\ ON \end{Bmatrix} \quad (1.8(b))$$

$$Sc = \begin{Bmatrix} 1\ if\ S3\ is\ ON\ and\ S6\ is\ OFF \\ 0\ if\ S3\ is\ OFF\ and\ S6\ is\ ON \end{Bmatrix} \quad (1.8(c))$$

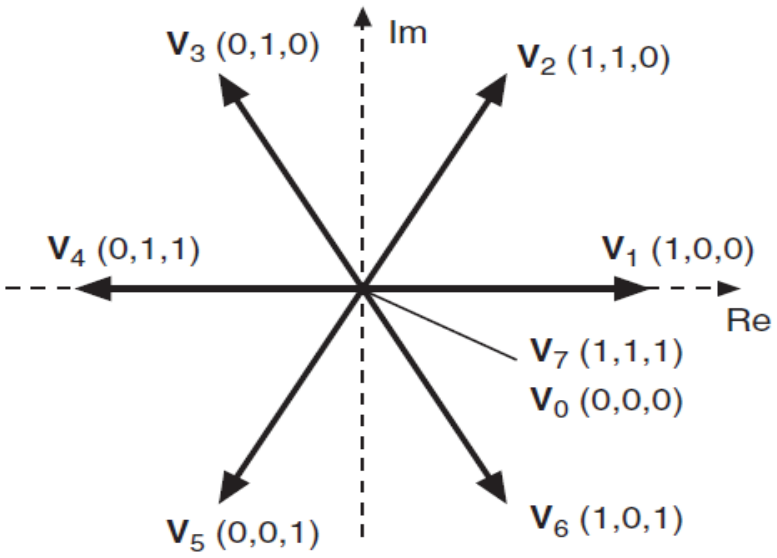

Fig.5. Different switching states for an inverter

In above equations the S1, S2, S3, S4, S5, S6 represents the six switches in the arms of the inverter as shown in Figure 6.

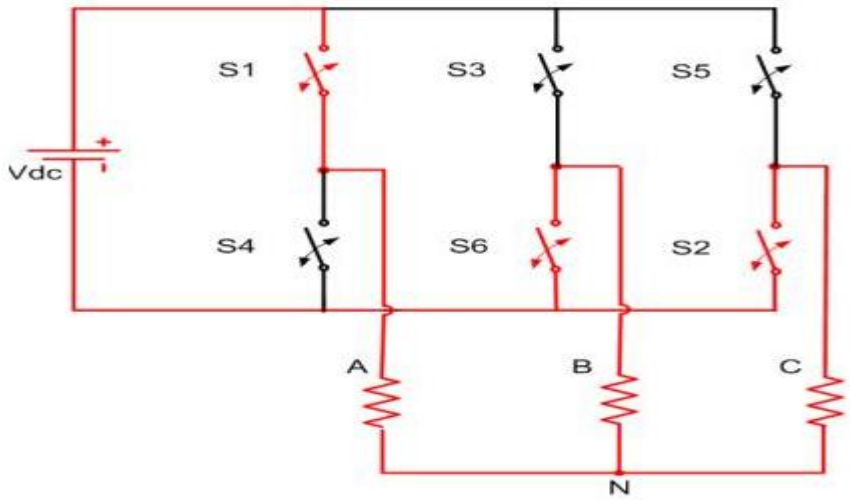

Fig.6. Simple circuit diagram of a 3 phase inverter

1.5. FIELD ORIENTED CONTROL SCHEME

In field oriented control the basic principle is same that is the 3 phase current and voltage are measured and then transformed into 2 phase voltage and current by Clarke and Park transformation. The reference value of Id is calculated by applying a PI control which is fed with the error in speed[13,17,47,9]. The output of PI controller gives the torque and from this value I_q is calculated by the relation given in equation 1.9.

$$Iq = \frac{2}{3}.\frac{2}{p}.\frac{L_r}{L_m}\frac{T_e}{\Psi} \tag{1.9}$$

In above equation L_r is the rotor inductance, L_m is the mutual inductance, T_e is the electrical torque and Ψ represents the calculated flux.

From reference flux I_d is calculated which is given in equation 1.10

$$Id = \frac{\Psi}{L_m} \tag{1.10}$$

Now these two phase values are converted into 3 phase currents and then a hysteresis current controller is fed with the error between the reference and measured values of three phase currents. Output of hysteresis current controller provides the switching for inverter from which the Induction Motor is controlled. Figure 7 shows the block diagram of Field Oriented Control (FOC).

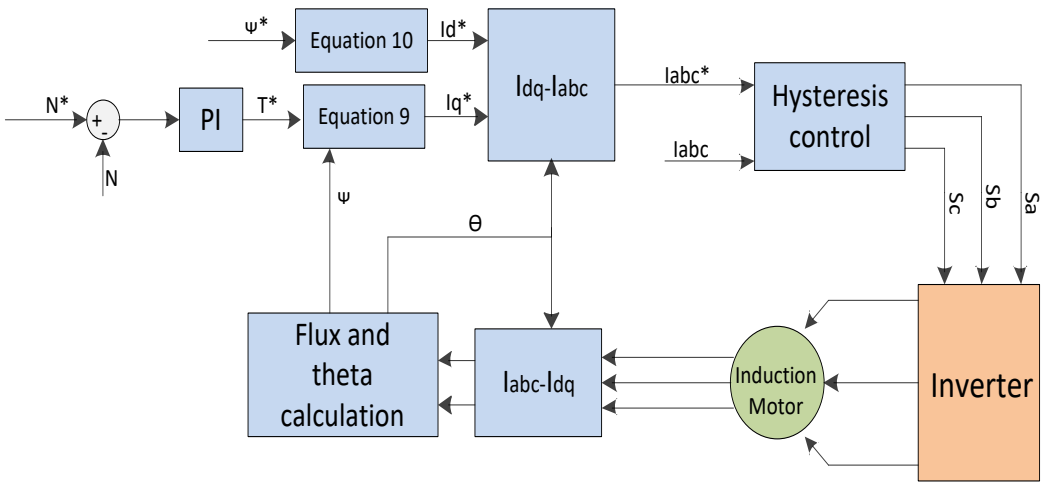

Fig.7. Block diagram for Direct Field Oriented Control

From classification we know that the Field Oriented Control (FOC) is further subdivided into two methods i.e Direct FOC and Indirect FOC. Figure 7 is showing the Direct FOC as the measured speed is directly sensed through the tacho-generator and then compared to the reference. Due to the need of the tacho-generator for Direct FOC, this approach becomes bulkier and costly. To remove tacho-generator, Indirect FOC is implemented in which the speed is also estimated from terminal voltage and currents and the only component which have to be measured from the motor terminals are only 3 phase voltages and currents.

1.6. ESTIMATION OF FLUX IN VECTOR CONTROL OF INDUCTION MOTOR

As discussed above in two schemes of Vector Control i.e Direct Torque Control and Indirect Field Oriented Control, the part from where the controlling action starts is the estimation of flux and rotor angle θ. Estimation part of any controlling scheme is very important. In these two schemes also the estimation of rotor flux is done. The two methods for estimating the rotor flux are:

1) Current model based estimation of rotor flux
2) Voltage model based estimation of rotor flux

In current model the estimation is done by using the rotor parameters i.e rotor resistance, rotor inductance, and mutual inductance along with the terminal voltages and currents, because of this the current model is not reliable because the rotor parameters change with the performing conditions of the Induction Motor. On the other hand the voltage model estimation for flux is done by using only one parameter of Induction Motor i.e stator resistance along with the terminal voltages and currents. The stator resistance remains almost constant during transient and steady state operation of Induction Motor with very wide range of speed. The main problem associated with the current model based estimation of rotor flux is that of the parameters used in the model. These models are mostly the rotor parameters which are likely to change with the change in running conditions of the motor. So, the estimation will not be accurate. If the flux estimation is not accurate this may lead to the wrong switching state of the inverter which will effect the performance of Induction Motor. Voltage model on the other hand uses only one parameter of induction model i.e the stator resistance which does not change and remains almost constant in all driving conditions of the motor.

In voltage model the flux is basically estimated by integrating the back emf of the motor. The back emf of the motor is calculated by equation 1.11 and the estimated rotor flux can be obtained from equation 1.12.

$$emf = V - I.R_s \tag{1.11}$$

$$\Psi = \int emf = \int (V - I.R_s) \tag{1.12}$$

where V,I represents terminal voltage and current respectively and R_S represents the stator resistance.

1.7. PREDICTIVE CONTROL

Model Predictive Control (MPC) is an advanced method of process control that has been in use in the process industries in chemical plants and oil refineries since the 1980s. In recent years it has also been used in power system balancing models Model predictive controllers rely on dynamic models of the process, most often linear empirical models obtained by system identification. The main advantage of MPC is the fact that it allows the current timeslot to be optimized, while keeping future timeslots in account. This is achieved by optimizing a finite time horizon, but only implementing the current timeslot. MPC has the ability to anticipate future events and can take control actions.PID and LQR controllers do not have this predictive ability[10,12].

MPC is nearly universally implemented as a digital control. Model predictive control uses a mathematical model to simulate a process. This model then fits the inputs to predict the system behavior. In this way, MPC is a type of feed forward control. It uses system inputs as a basis of control. MPC is more complex than most other feed forward control types because of the way these predictions are used to optimize a process over a defined amount of time. Most feed forward control types do not take into account the process outputs much past a

residence time. The MPC algorithm will compare predicted outputs to desired outputs and select signals that will minimize this difference over the time selected. The main algorithm used for applying Predictive control in Induction Motor controlling is discussed in chapter 4.

1.8. MOTIVATION

The problem associated with this estimation is related to the pure integrator. In pure integration if a sinusoidal wave is given in the input the output must be a cosine with same frequency and if the frequency of input is given 1 rad/sec, then the output cosine must be of the same magnitude as the sinusoidal input. In pure integration this is true only if the sinusoidal input is given at the instants where it achieve its positive or negative peaks, otherwise a dc offset appears at the output of the integrator, this problem is called the **initial value problem.** Another major problem associated with the pure integrator is that if dc offset is present along with the sinusoidal input then the output of the integrator will keep increasing and finally drive the integrator into **saturation**. The main aim this thesis is to discuss various algorithms to remove these problems associated with pure integration and to discuss the working, advantages and disadvantages of the algorithms.

In the vector control of Induction Motor the error between the reference current and the terminal currents are fed to the hysteresis controller. In place of hysteresis control a Model Predictive Controller is implemented and the results are obtained for Direct Vector Control of Induction Motor model.

1.9. ORGANIZATION OF THESIS

Chapter 2 describes the modeling of Induction Motor along with the DTC and FOC. In chapter 3 various filters to compensate the problems associated with the pure integration are discussed along with their working. In chapter 4 the implementation of these algorithms on the DTC drive is done on the **simulink MATLAB.** In chapter 5 Model Predictive Control based simulation is done on the Direct Vector Control of Induction Motor. In chapter 6 the results and discussion is done and in chapter 7 conclusion and future scope is drawn.

CHAPTER 2

MODELLING OF INDUCTION MOTOR

2.1. INDUCTION MOTOR MODELLING FOR VECTOR CONTROL

Vector control of Induction Motor is used for high performance Induction Motors. As we know that vector control is used for Induction Motor to obtain the performance equivalent to DC motor. Now for obtaining this we have to find two current components, in which one is responsible for flux and other is responsible for torque.

So, we have to find the current which is proportional to Torque, and the flux Ψ which is orthogonal to torque producing component. Now the Ψ generated by current I, but for Induction Motor current is vector sum of Ψ producing component and torque producing component are shown in Figure 8[20.46,47].

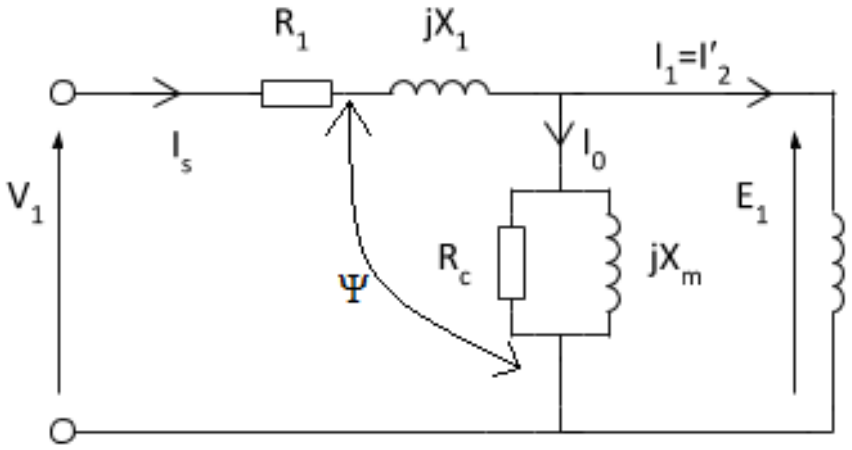

Fig.8. Diagram showing the direct field oriented control

In Figure 8, Ψ represents the total flux component and I_0 represents the rotor flux producing component and I_2 represents the torque producing component. Figure 9 represents

the phasor diagram representing the total flux component I_s, magnetic current I_m, and torque producing component I_r. The reference for phasor diagram in Figure 9 is taken as Ψ_m, I_Ψ is the component in the direction of pure inductance and I_r is in the direction of resistance and inductance.

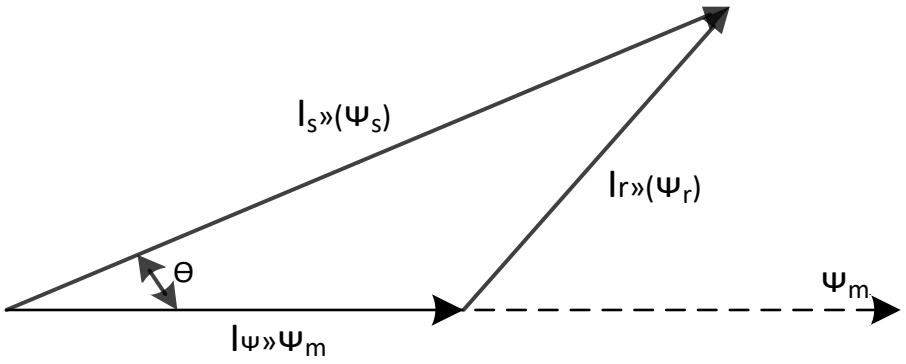

Fig.9. Phasor diagram for Induction Motor

Now as we now that emf induced is the n times the rate of change of flux, so voltage across R_r/s is given by equation 2.1.

$$Voltage\ across\ \frac{Rr}{s} = \frac{d\Psi r}{dt} = j.\omega.\Psi r.\cos\omega t \qquad (2.1)$$

Now we have to divide this total component I_s into two components, and according to this dynamic model must be developed, under dynamic conditions current values can change. Now if we want to resolve the current 'I_s' along Ψ_r and perpendicular to it, we need to know the position of Ψ_r under all dynamic condition. This is the basic concept of Vector Control of Induction Motor.

Now by Clarke transformation three phase quantities (abc) are changed to αβ component which is the stationary frame of reference given by equation 2.2(a) and 2.2(b) .

$$I_s = I_\alpha + j.I_\beta \qquad 2.2(a)$$

$$V_s = V_\alpha + j.V_\beta \qquad 2.2(b)$$

α-axis is always placed at the a phase axis. Equation 2.2(a) and 2.2(b) can be represented by 2.3(a) and 2.3(b). Now in steady state these phases rotate that is ϕ rotate and angles are fixed between voltage and currents and in dynamic model ϕ and magnitude both varies.

$$I_s = |I_s|.e^{j.\omega.t} \qquad 2.3(a)$$

$$V_s = |V_s|.e^{j.\omega.t} \qquad 2.3(b)$$

Figure 10 shows phasor for stationary frame of reference. The stator and rotor equations are given by equation 2.4and 2.5.

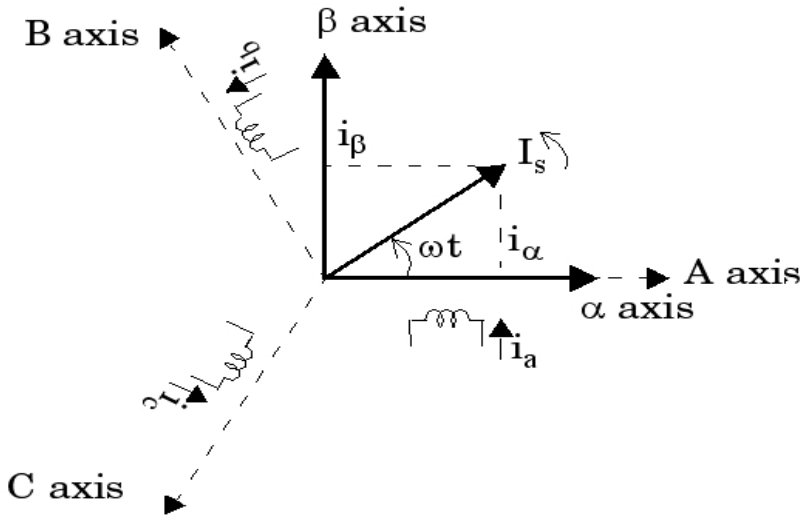

Fig.10. Phasor diagram for αβ frame of reference

For stator

$$V_s = R_s.I_s + L_{ss}.\frac{dI_s}{dt} + M.\frac{dI_r}{dt} \qquad (2.4)$$

For rotor (rotor is shorted in IM so net voltage sum across the mesh is equal to zero)

$$0 = R_r.I_r + L_{rr}.\frac{dI_r}{dt} + M.\frac{dI_s}{dt} \qquad (2.5)$$

Now we want to find instantaneous position of rotor flux for converting αβ into dq reference frame i.e synchronous frame of reference. So, if we know the instantaneous position of ϕ_R i.e the rotor flux , then we can position dq along ϕ_r.

Figure 11 shows the shifting of αβ reference frame to dq reference frame, here θ shows the rotor angle and ϕ_1 and ϕ_2 shows angle with I_s and V_s with respect to stationary reference frame axis α.

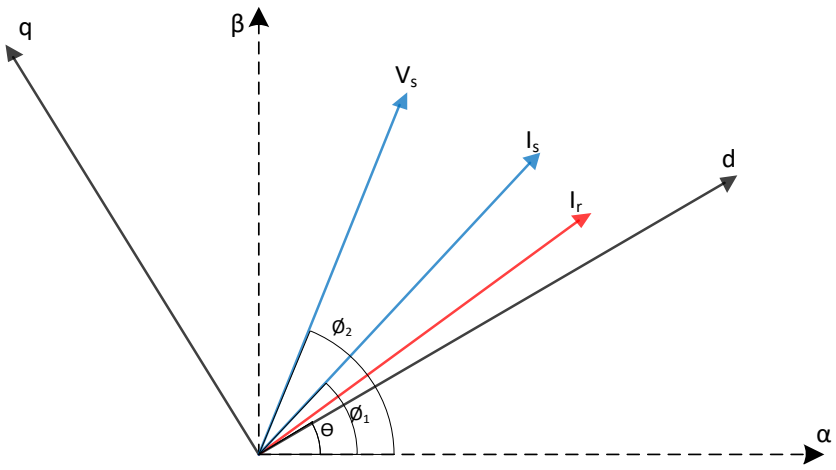

Fig.11. Phasor diagram for dq frame of reference

Now for transforming voltages and currents from stationary frame of reference to synchronous frame of reference equation 2.6(a), 2.6(b), 2.7(a) and 2.7(b) are used[37].

$$V_{sd} = |V_s|.\cos(\phi_1 - \theta) \quad (2.6(a))$$

$$V_{sq} = |V_s|.\sin(\phi_1 - \theta) \quad (2.6(b))$$

$$I_{sd} = |I_s|.\cos(\phi_2 - \theta) \quad (2.7(a))$$

$$I_{sq} = |I_s|.\sin\ (\phi_2 - \theta) \quad (2.7(b))$$

Now the final dynamic equations for stator and rotor with dq frame of reference are given in equation 2.8(a), 2.8(b), 2.9(a) and 2.9(b).

For stator d axis voltage equation

$$V_{sd} = R_s.I_{sd} + L_{ss}.\frac{dI_{sd}}{dt} - L_{ss}.\omega_\theta.I_{sq} + M.\frac{dI_{rd}}{dt} - M.\omega_\theta.I_{rq} \qquad (2.8(a))$$

For stator Q axis voltage equation

$$V_{sq} = R_s.I_{sq} + L_{ss}.\frac{dI_{sq}}{dt} - L_{ss}.\omega_\theta.I_{sd} + M.\frac{dI_{rq}}{dt} - M.\omega_\theta.I_{rd} \qquad (2.8(b))$$

For rotor d axis voltage equation

$$0 = R_r.I_{rd} + L_{rr}.\frac{dI_{rd}}{dt} - L_{rr}.(\omega_\theta - \omega_r).I_{rq} + M.\frac{dI_{sd}}{dt} - M.(\omega_\theta - \omega_r).I_{sq} \qquad (2.9(a))$$

For rotor q axis voltage equation

$$0 = R_r.I_{rq} + L_{rr}.\frac{dI_{rq}}{dt} - L_{rr}.(\omega_\theta - \omega_r).I_{rd} + M.\frac{dI_{sq}}{dt} - M.(\omega_\theta - \omega_r).I_{sd} \qquad (2.9(b))$$

In above equations

Stator inductance=Lss= M+Ls, where M is mutual inductance and Ls is stator self inductance

Rotor inductance=Lrr= M+Lr, where M is mutual inductance and Lr is rotor self inductance

ω_θ = Angular frequency with which dq axis is rotating

ω_r = Angular frequency of rotor

Vsd and Vsq = Stator voltages correspond to d and q axis

Isd and Isq= Stator currents correspond to d and q axis

Ird and Irq= Rotor currents correspond to d and q axis

Rr and Rs are rotor and stator resistance

Now based on the above equations the equivalent dynamic model is shown in Figure 12 and Figure 13.

D circuit equivalent model

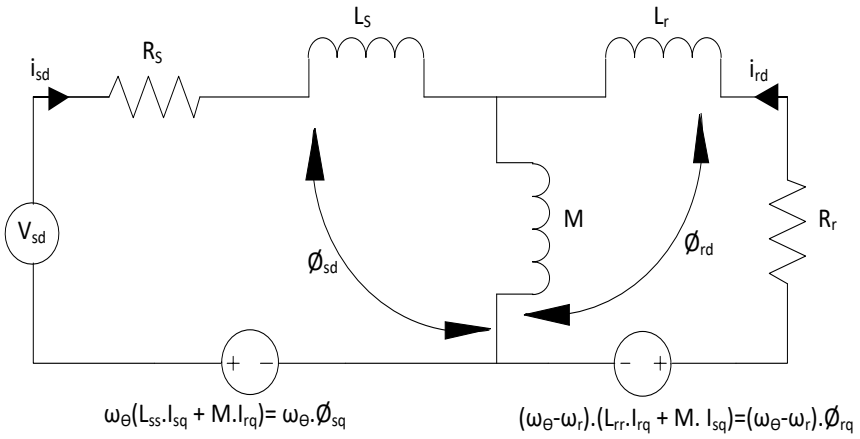

Fig.12. Equivalent dynamic model representing equation 20(a)

Q circuit equivalent model

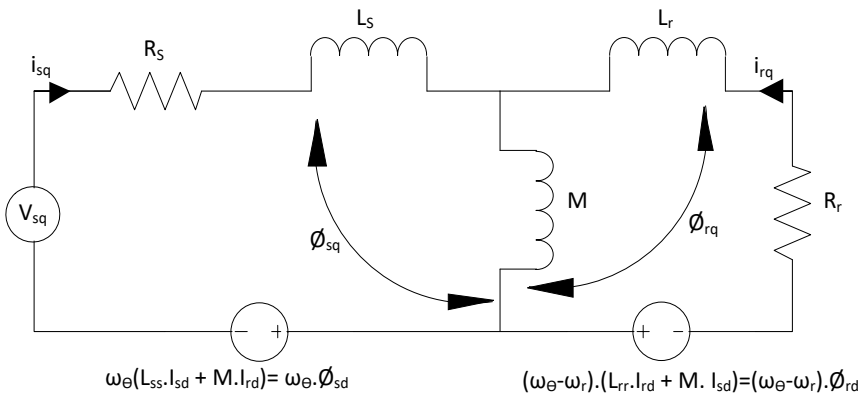

Fig.13. Equivalent dynamic model representing equation 20(b)

In above Figures ϕ_{sq} , ϕ_{rq} , ϕ_{sd} , ϕ_{rd} are given below:

$$\phi_{sq} = \omega_\theta\left(L_{ss}I_{sq} + M.I_{rq}\right) \quad (2.10(a))$$

$$\phi_{rq} = (\omega_\theta - \omega_r).\left(L_{rr}I_{rq} + M.I_{sq}\right) \quad (2.10(b))$$

$$\phi_{sq} = \omega_\theta(L_{ss}I_{sd} + M.I_{rd}) \quad (2.10(c))$$

$$\phi_{rd} = (\omega_\theta - \omega_r).(L_{rr}I_{rd} + M.I_{sd}) \quad (2.10(b))$$

Here dq axis is rotating with speed $\omega_{\theta,}$ so when ω_θ is zero then it represents the stationary reference frame and when ω_θ is equal to synchronous speed then it represents the synchronous reference frame.

So all the above equations can be represented in matrix form and given by equation 2.11.

$$\begin{bmatrix} V_{ds} \\ V_{qs} \\ 0 \\ 0 \end{bmatrix} = \begin{bmatrix} R_{ss} + L_{ss}.D & -\omega_s.L_{ss} & M.D & -M.\omega_s \\ L_{ss}.\omega_s & R_{ss} + L_{ss}.D & M.\omega_s & M.D \\ M.D & -(\omega_s - \omega_r).M & R_r + L_{rr}.D & -L_{rr}.(\omega_s-\omega_r) \\ -M.(\omega_s-\omega_r) & M.D & L_{rr}.(\omega_s-\omega_r) & R_{rr} + L_{rr}.D \end{bmatrix}.\begin{bmatrix} I_{ds} \\ I_{qs} \\ I_{dr} \\ I_{qr} \end{bmatrix} \quad (2.11)$$

Now power equation is given by equation 2.12. As we know that if we transform into any reference frame then in any reference frame power balance should be met, so for this a factor of 2/3 is multiplied to power equation.

$$Power(P) = \frac{2}{3}.\frac{M\omega_s}{L_{rr}}\left(\phi_{rd}.I_{sq} - \phi_{rq}.I_{sd}\right) \quad (2.12)$$

Now as we know that torque is power divided by angular speed so torque equation is given by equation 2.13.

$$Torque(T) = \frac{2}{3}.\frac{P}{2}.\frac{M}{L_{rr}}\left(\phi_{rd}I_{sq} - \phi_{rq}.I_{sd}\right) \quad (2.13)$$

For Field Oriented Control, we want that ϕ_r i.e the resultant flux should always align along d axis. So, for this ϕ_{rq} must be equal to zero, now by putting ϕ_{rq} equal to zero in above torque equation we get equation 2.14, so from equation 2.14 we can see that torque is directly proportional to I_{sq} as given in equation 2.15. So the total flux ϕ_R is equal to ϕ_{sd} which can be controlled by the current component I_{sd} and the component perpendicular to it is I_{sq}, and by varying it Torque can be controlled as torque is directly proportional to $\phi_{sq,}$ and finally a decoupled action is obtained.

$$Torque(T) = \frac{2}{3}.\frac{P}{2}.\frac{M}{L_{rr}}.\left(\phi_{rd}I_{sq}\right) \quad (2.14)$$

$$Torque(T) \propto I_{sq} \quad (2.15)$$

So, it can be established that by varying the orthogonal component i.e perpendicular component I_{sq} the developed torque control is possible.

As we have established above that ϕ_{qr} should be equal to zero in Vector Control,we can write

$$\phi_{qr} = 0$$

$$\frac{d\phi_{qr}}{dt} = 0$$

So from equivalent Q circuit model, and taking $\omega_\theta = \omega_s$ we can write

$$(\omega_s - \omega_r).\phi_{rd} + R_r I_{rq} = \frac{d\phi_{qr}}{dt} = 0 \quad (2.16)$$

and $$M.I_{sq} + L_{rr} I_{rq} = \phi_{qr} = 0 \quad (2.17)$$

From equation 2.16 and 2.17 we can establish a relation with ω_{slip} and I_{sq} which is given by equation 2.18.

$$(\omega_s - \omega_r).\phi_{rd} = R_r I_{qs}.\frac{M}{L_{rr}}$$

$$\omega_{slip}\phi_{rd} = \frac{M}{L_{rr}}.I_{sq}.R_r \quad (2.18)$$

So now from above equation we can say that ω_{slip} is directly proportional to I_{sq}.

Now from equivalent d axis model the term $(\omega_s - \omega_r).\phi_{rd}$ will be equal to zero.

By keeping constant I_{sd} we are keeping ϕ_{rd} constant.

Now again as we established earlier that ϕ_{qr}=0 for vector control so total flux ϕ_r is equal to ϕ_{dr}.

$$\phi_r = \phi_{dr} = M.I_{ds} + L_{rr}.I_{dr}$$

Here we define, $\sigma_r = \frac{L_{rr}-M}{M}$, so we can write the above equation as

$$\phi_{dr} = M.I_{ds} + M.(1+\sigma_r).I_{dr} \quad (2.19)$$

Again ϕ_{dr}= M.I_{dr}

so from equation 2.19 we can have I_{dr} as

$$I_{dr} = \frac{(I_{mr}-I_{ds})}{1+\sigma_r} \quad (2.20)$$

Now from rotor side

$$\frac{d\phi_{dr}}{dt} + R_r I_{dr}$$

$$\frac{M(1+\sigma_r)}{R_r}.\frac{dI_{mr}}{dt} + R_r\frac{(I_{mr}-I_{ds})}{1+\sigma_r} = 0$$

$$\frac{M(1+\sigma_r)}{R_r}.\frac{dI_{mr}}{dt}+I_{mr}=I_{ds}$$

Now as we established I_{mr} is constant as we want to have a constant flux, so that makes

$$I_{mr}=I_{ds} \tag{2.21}$$

So from equation 2.18 we can write

$$I_{mr}=I_{ds}=\frac{M}{\omega_{slip}.L_{rr}}.I_{sq}.R_r \tag{2.22}$$

R_r/L_{rr} can be written as time constant τ_r , so we can finally write

$$\omega_{slip}=\frac{I_{sq}}{\tau_r.I_{sd}} \tag{2.23}$$

As we know in Induction Motor we can write a mechanical equation as in equation 2.24 where T_d represents developed torque, T_l represents load torque, J represents moment of inertia and ω represents angular speed of Induction Motor.

$$T_d-T_l=J.\frac{d\omega}{dt} \tag{2.24}$$

Now from all the discussion and modeling equations of Induction Motor for vector control a final block diagram showing the Field Oriented Control scheme of Induction Motor is shown in Figure 14 and 15.

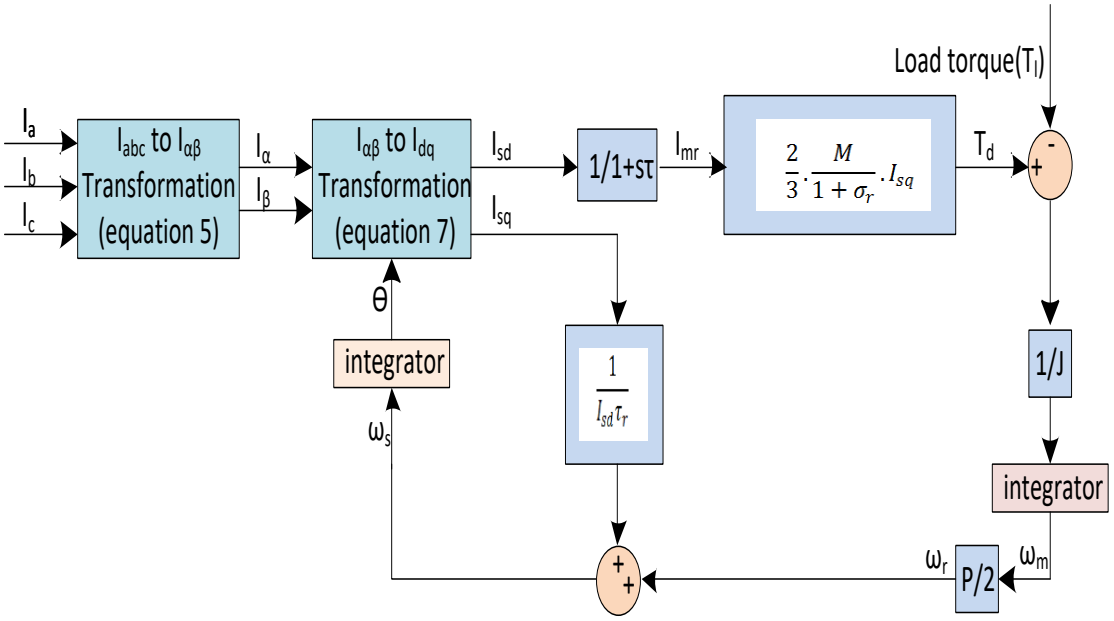

Fig.14. Induction Machine model under Field Oriented Control

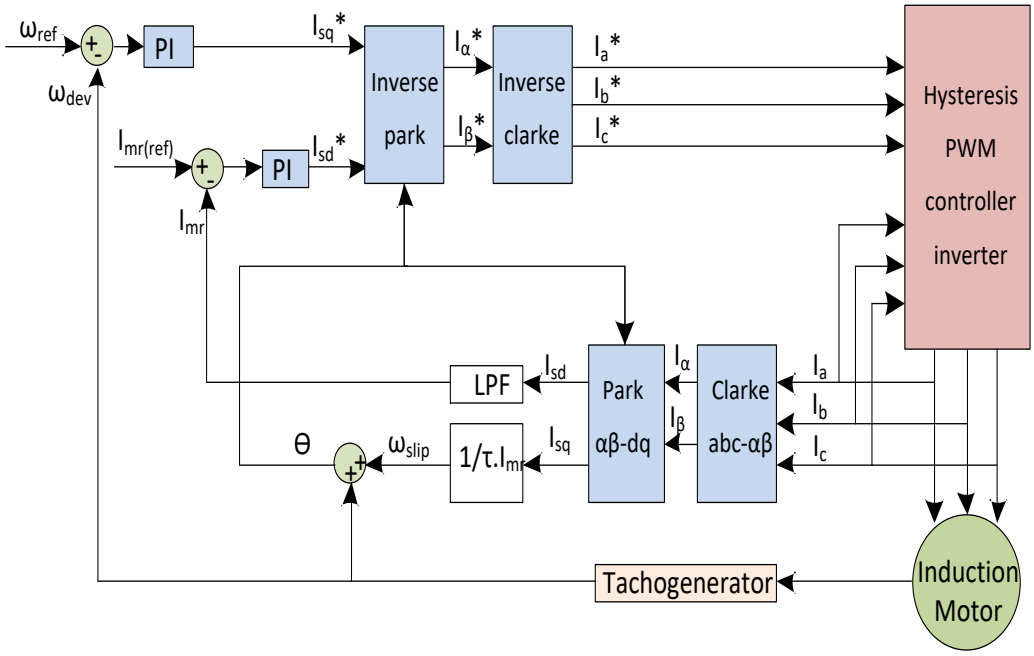

Fig.15. Block diagram for Direct Field Oriented Control

2.2. FLUX ESTIMATION MODELS

As it was discussed in first chapter that for flux estimation in Induction Machine two models can be used namely Current Model for Flux Estimation and Voltage Model for Flux Estimation[46].

2.2.1. Current model

The equations for the current model for estimating the flux of Induction Motor are given by equation 2.25 and 2.26, and Figure 16 shows the block diagram for current model estimation.

$$\frac{d\Psi_{dr}}{dt} = \frac{L_m}{\tau_r} I_d - \omega_r . \Psi_{qr} - \frac{1}{\tau_r} \Psi_{dr} \tag{2.25}$$

$$\frac{d\Psi_{qr}}{dt} = \frac{L_m}{\tau_r} I_q - \omega_r . \Psi_{dr} - \frac{1}{\tau_r} \Psi_{qr} \tag{2.26}$$

where $\tau_r = L_r/R_r$

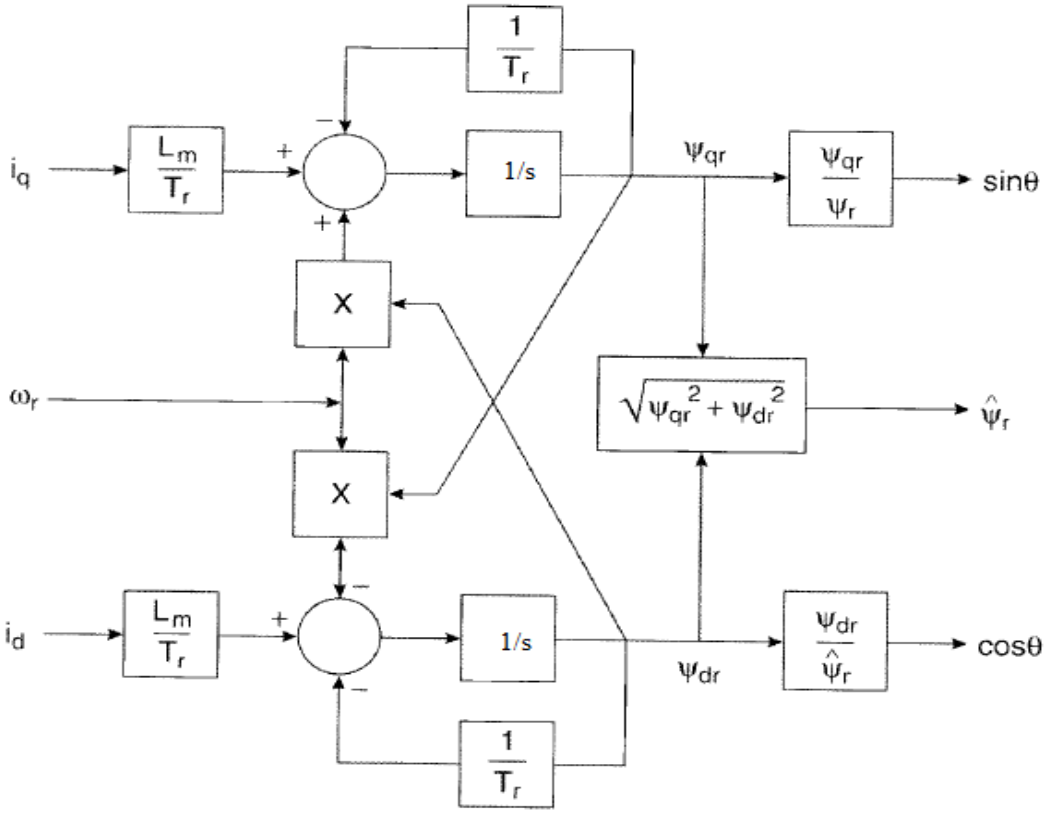

Fig.16. Block diagram for current model estimation of flux

Now as we can see from equations and block diagram that this model depends on the rotor parameters, which can change with the operating condition of Induction Motor, so this model is not reliable.

2.2.2. Voltage model

The simple equations for voltage model based estimation of flux are given by equations 2.27 and 2.28.

$$\Psi_{ds} = \int V_{ds} - I_{ds}.R_s \tag{2.27}$$

$$\Psi_{qs} = \int V_{qs} - I_{qs}.R_s \tag{2.28}$$

The block diagram showing the voltage model flux estimation scheme is shown in Figure 17.

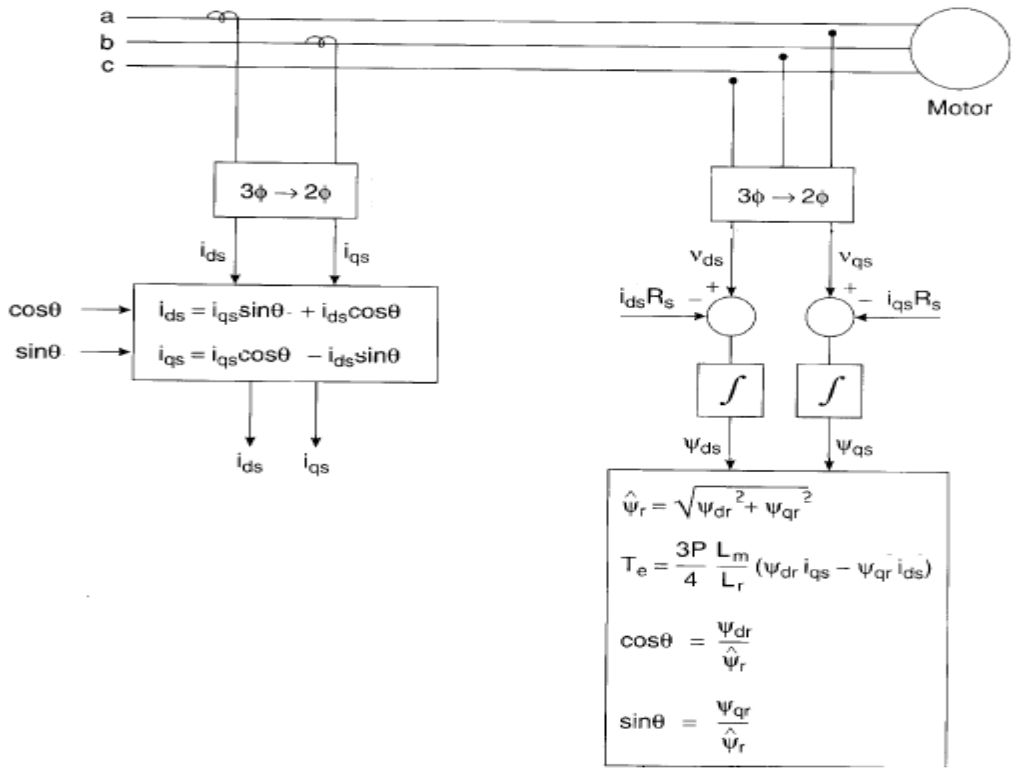

Fig.17. Block diagram for voltage model estimation of flux

From above equations and block diagram it is clear that for flux estimation with voltage model only one parameter is needed that is stator resistance which remains almost constant in wide range of operating conditions of the Induction Motor.

CHAPTER 3

FILTER DESIGNING

3.1. PURE INTEGRATOR THEORY

If we apply a sinusoidal quantity at the input of pure integrator the result must be cosine with same frequency. In pure integrator however applying a sine will give cosine only at two instants, i.e at the instants where the sinusoidal quantity achieves its positive or negative peak values[2,4].

Let us assume a signal X with amplitude A_m which is sinusoidal in nature which is to be integrated and gives output Y as given in equation 3.1.

$$Y = \int X.dt \tag{3.1}$$

For $X = Am\sin(\omega t)$, then

$$Y = \frac{1}{\omega}(-Am.\cos(\omega t) + Am.\cos(\omega t)\Big|_{t=0})$$

$$Y = \frac{1}{\omega}(-Am.\cos(\omega t) + Am) \tag{3.2}$$

As it can be seen from equation 3.2 that at the output of the integrator a constant dc offset is present which appears due to the initial value of the limit of integrations i.e taking t=0 as the initial point.

If we consider a signal which is having a measurement offset at input A_{dc}

For $X = Am\sin(\omega t) + A_{dc}$, then

$$Y = \frac{1}{\omega}(-Am.\cos(\omega t) + Am.\cos(\omega t)\big|_{t=0}) + A_{dc}t - A_{dc}t|_{t=0} \quad .$$

$$Y = \frac{1}{\omega}(-Am.\cos(\omega t) + Am) + A_{dc}t \tag{3.3}$$

Now if we compare Equation 3.2 and 3.3 then we can observe that in equation 3.3 there is an additional term present that is of ramp nature, so due to the offset errors present in input the integrator is derived to the saturation. So while implementing integrator in an estimation scheme if their present a measurement offset value or offset value due to any other reason, then estimation scheme will not work properly as integrator will be saturated no matter how small is the offset at input. It is to be noticed that if the sinusoidal input is applied at the instants where it achieve the positive or negative peaks then there will be no initial value error at the output, but it is not always possible. Figures 18(a) and 18(b) shows the pure integrator output when sinusoidal input is applied and Figure 19(a) and 19(b) shows the output of integrator when input is applied at the peaks[40].

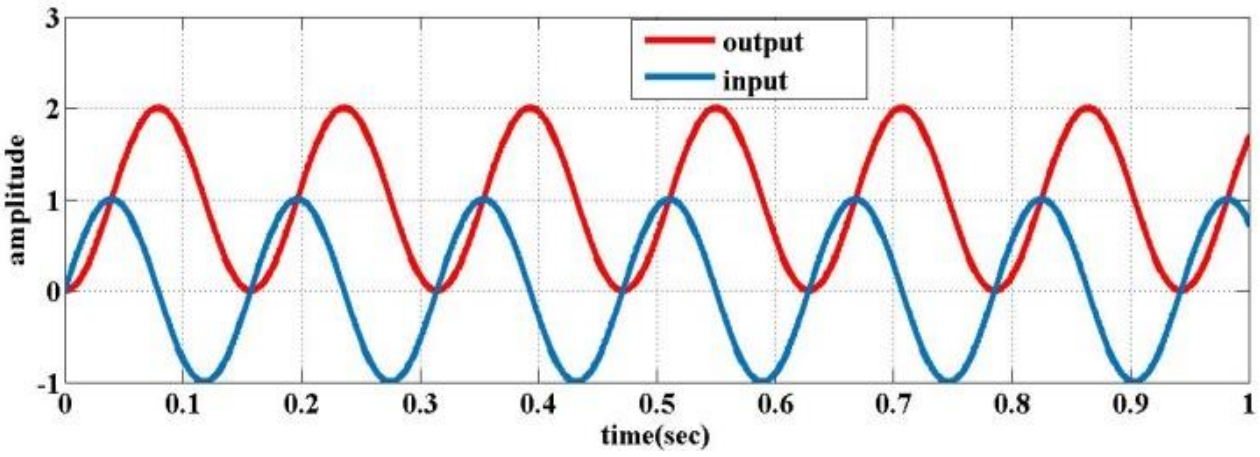

Fig.18(a). Error due to initial value problem

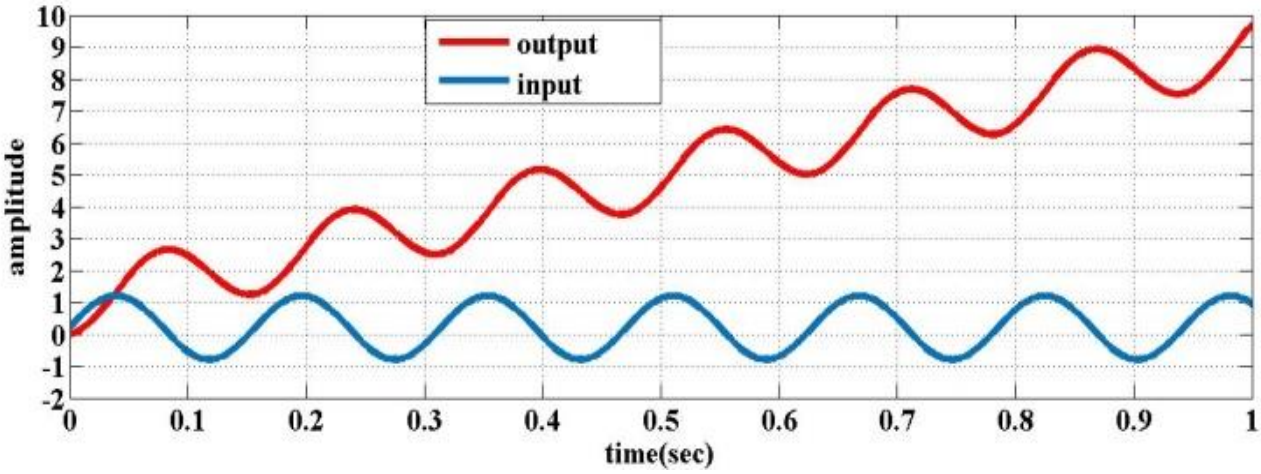

Fig.18(b). Error due to measurement offset at the input

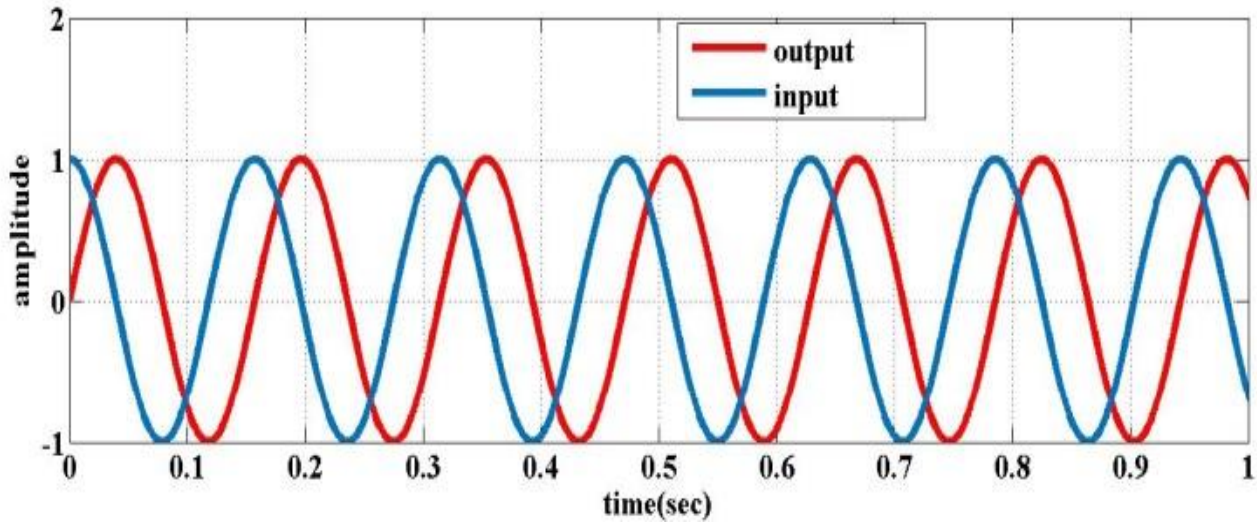

Fig.19(a).Output when applied at peak, no initial value error

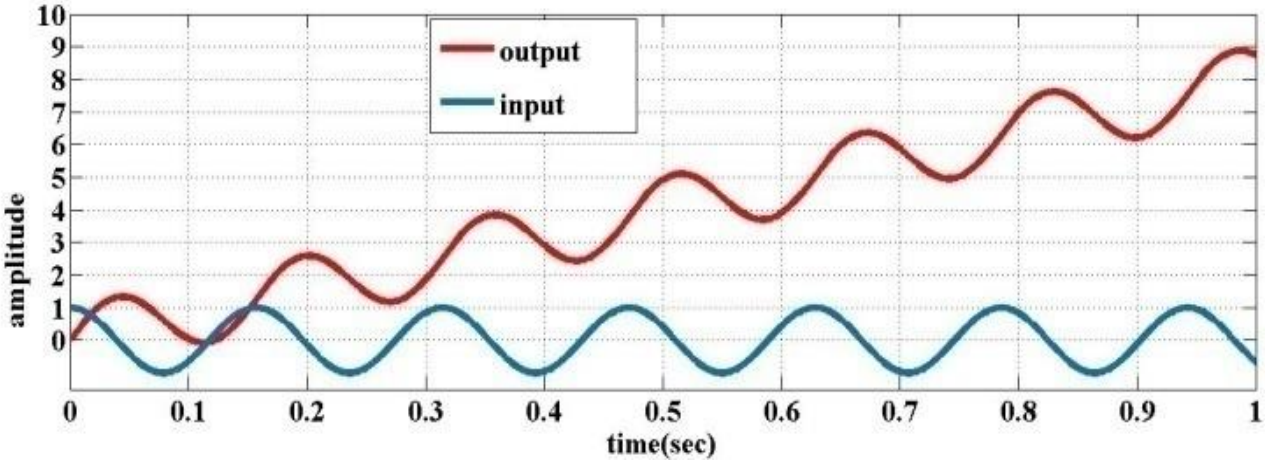

Fig.19(b).Output when applied at peak, measurement offset errors persist

3.2. LOW PASS FILTER

Now to compensate the initial value problem that gives an offset at the output and measurement offset problem that drives the integrator into saturation a low pass filter is proposed in place of the pure integrator in controlling scheme. Figure 3 shows the block diagram of the Low Pass Filter[1,5,40].

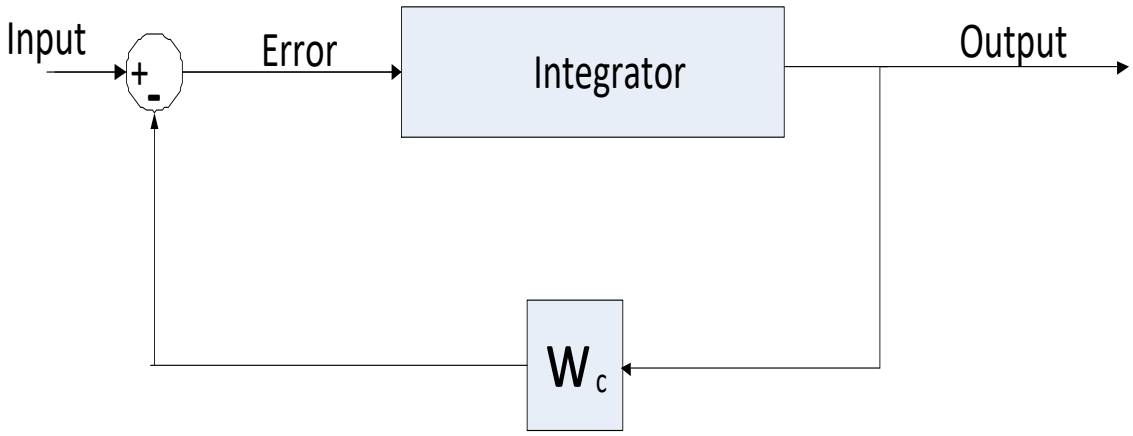

Fig.20. Block diagram of a low pass filter

TABLE I. Magnitude and Phase errors introduced by Low Pass Filter

	MAGNITUDE	PHASE
PURE INTEGRATOR	$\frac{1}{\omega}$	$\frac{-\pi}{2}$
LOW PASS FILTER	$\frac{1}{\sqrt{{\omega_C}^2 + {\omega_s}^2}}$	$-\tan^{-1}\frac{\omega_S}{\omega_c}$

For reducing the drift problems associated with the pure integrator it should be taken care that the cut off frequency of the low pass filter must be fixed lesser to the input frequency. If the cut off frequency chosen equal to or higher than input frequency it will introduce errors and if the chosen frequency is very less than supply frequency then it must be noted that

effectiveness of the low pass filter will be reduced as it will be approximated as pure integrator.

But by replacing pure integrator with LPF introduce magnitude and phase errors given in table 1. The phasor diagram of LPF and pure integrator is shown in Figure 21.

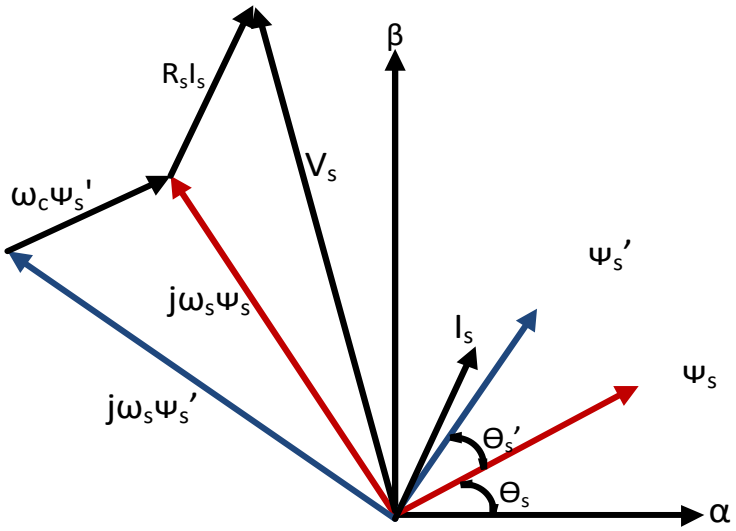

Fig.21. Phasor diagram of LPF

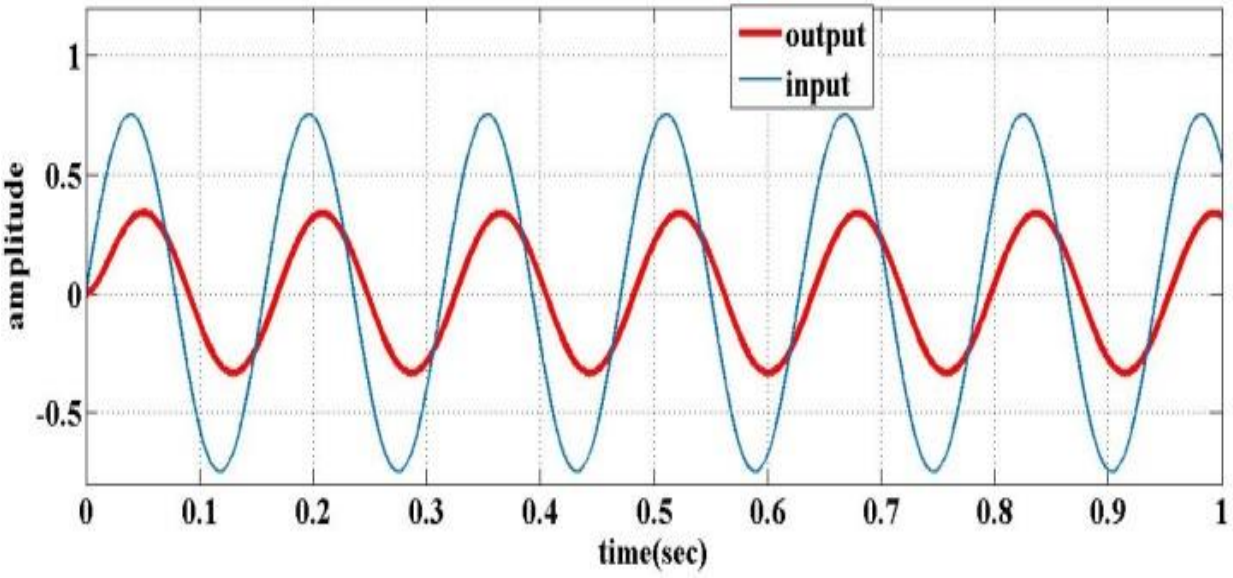

Fig22(a). LPF with cut off frequency higher than input frequency

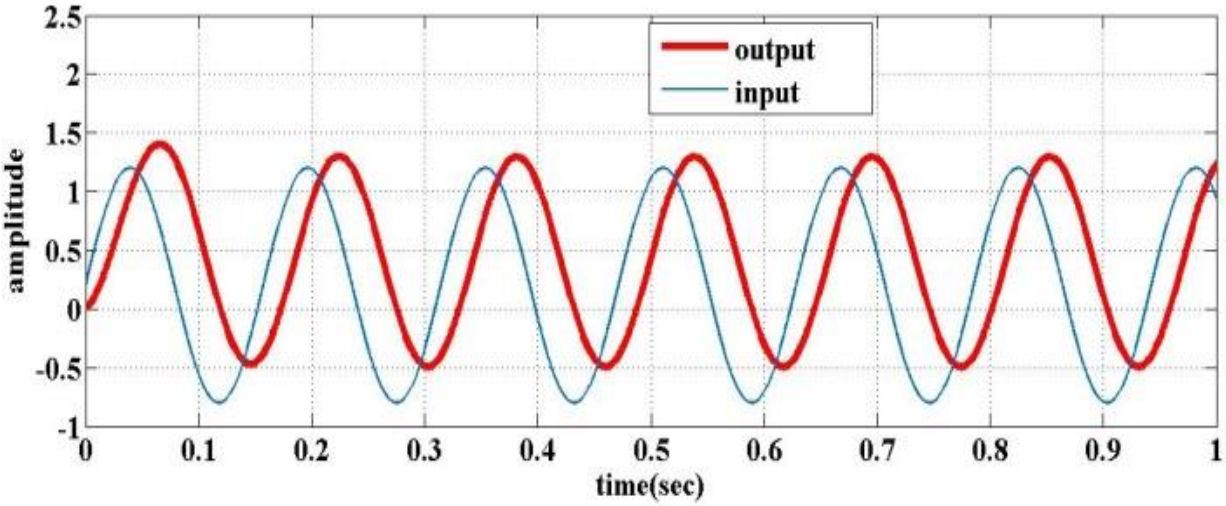

Fig22(b). LPF with cut off frequency lower than input frequency

Figure 22(a) shows the output of integrator when cut off frequency is selected higher than input frequency, which introduce huge amount of phase and magnitude errors. Figure 22(b) shows the output when cut off frequency is selected lower than operating frequency. It can be seen that errors are reduced but drift problem persist. So, the cut off frequency must be chosen in a way so that to achieve a balance.

3.3 ALGORITHMS FOR COMPENSATING INTEGRATION ERROR

3.3.1 Algorithm/Strategy 1(Calculating average in each cycle feedback)

The basic principle in this strategy is the fact that the average of a sinusoidal wave in a cycle is equal to zero. This strategy is used in applications where the time constant of the system is large and the offset present at the input terminal is small. This means the increase of the ramp type output will also be small. So a moving average is calculated of the output in every cycle and it is subtracted from it. Main advantage of using this strategy is that it uses pure integrator. Block diagram of this strategy is shown in Figure 23[6].

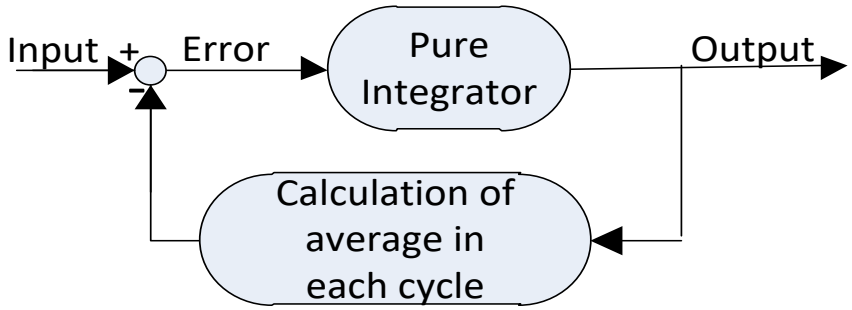

Fig.23. Block diagram for strategy 1

3.3.2 Algorithm/Strategy 2 (modified integrator of strategy 1 with compensation of input bias)

Strategy 1 is for the applications where the measurement offset at input is minimum however it is not the case every time. So, for these applications an another strategy is suggested where at the input compensation of offset is done by introducing a Low Pass Filter. The block diagram of this strategy is shown in Figure 24.Main drawback of strategy 1 and strategy 2 is that it only deals with the measurement offset problem and not with the initial value problem of the integrator. Also it can be seen in the results that the response of the modified integrators with strategy 1 and strategy 2 is not free from errors[6].

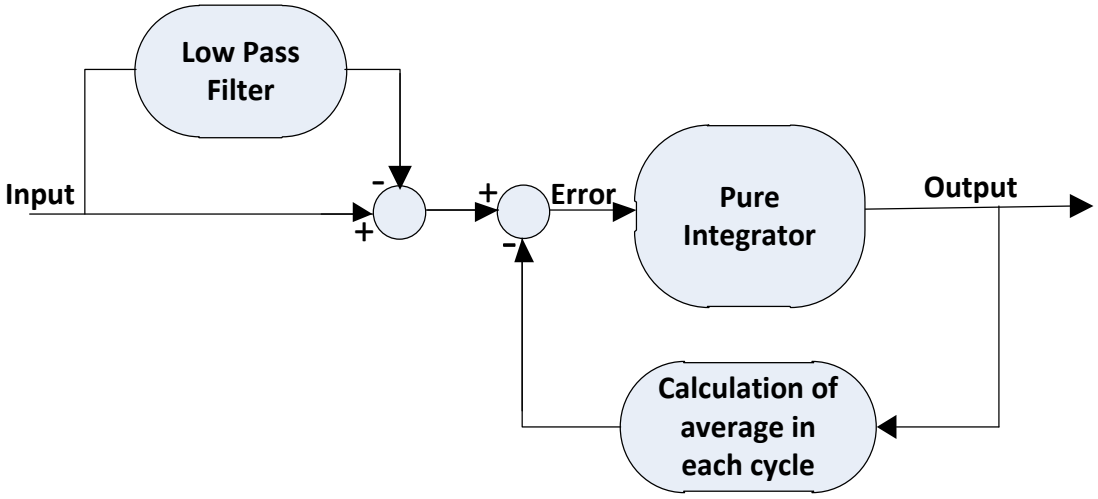

Fig.24. Block diagram for strategy 2

3.3.3 Algorithm/Strategy3 (Modified low pass filter with saturation feedback)

A pure integrator and low pass filter is discussed in section II. Strategy 3 is given by equation 3.4[3].

$$y = \frac{x}{1+\omega} + \frac{\omega . Z_{comp}}{1+\omega} \tag{3.4}$$

Here ω represents the cut off frequency and Z represents the compensation feedback as shown in Figure 25.

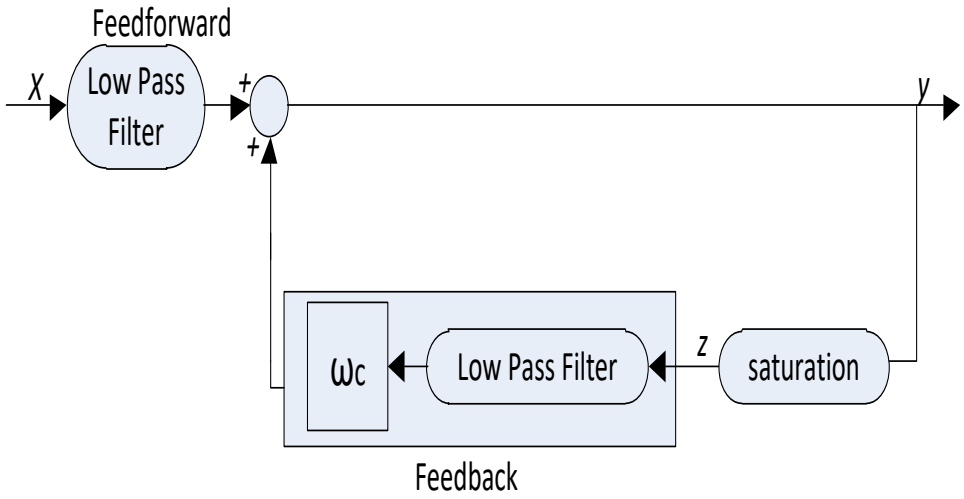

Fig.25. Block diagram for strategy 3

Equation 3.4 represents a modified integrator, if the value of Z is taken directly from the output i.e Z=y, then equation 4 act as a pure integrator, on the other hand if we put Z=0, equation 4 behave as a low pass filter, so by varying the saturation value at the feedback we can reduce the errors introduced by pure integration and as well as can reduce the phase and magnitude errors that are introduced by Low Pass Filter. The main problem with this strategy is to select the value of saturation.

In drive applications the error mainly comes when drive runs at very low speed, which means the operating frequency is low, in this scenario the measurement error is high as compared to integrator output which results in saturation of the integrator. For this strategy let us assume that a pure dc signal is applied at the input, then from equation 3.4 the maximum output is

$$y = \frac{x}{\omega} + L \tag{3.5}$$

where L is the limiting value provided at the fepath,from equation it can be implied that strategy 3 based modified integrator will not saturate provided limiting value of saturation is properly set. Limiting value should be set equal to the reference output needed as per the application.

For drive applications the limiting value of saturation must fixed equal to the reference flux value. If the limiting value is set more than reference flux value, then output flux waveform shifts upward or downward due to measurement dc offset at input, and it will increase until it reaches upper or lower limiting value. So, output flux waveform will contain an AC signal with a dc offset. If limiting value is set lower than the reference value then the output will not contain any dc offset but it will be distorted[32,39].

3.3.4 Algorithm/Strategy 4(Splitting magnitude and angle for control)

To eliminate the distortion problem of strategy 3 which is due to setting the limiting value less than the reference value a new integration algorithm is developed[3].

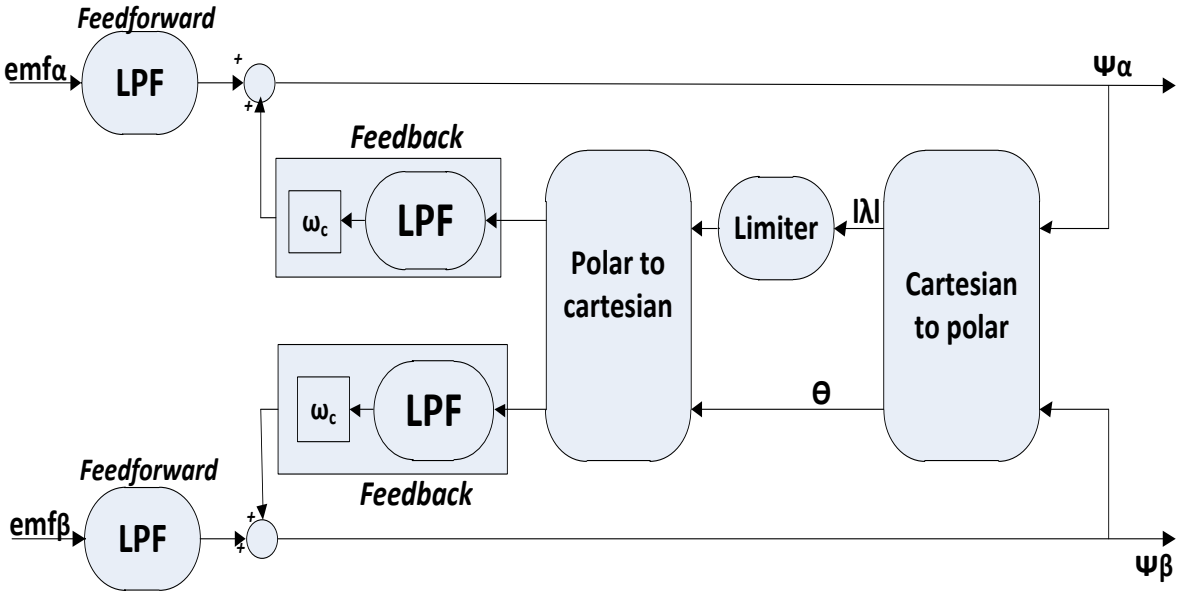

Fig.26. Block diagram for strategy 4

This is specially used for AC drive control system, because in ac drive vector control the three phase of terminal voltage and current are transformed to two phase quantities in αβ reference frame for controlling, the αβ flux is then calculated with these values. In strategy 4 the outputs Ψ_α and Ψ_β are converted to polar form where magnitude Ψm and phase angle θ is given by equation 3.6(a) and 3.6(b)[7,8].

$$\Psi m = \sqrt{\Psi\alpha^2 + \Psi\beta^2} \qquad (3.6(a))$$

$$\theta = \tan^{-1}\frac{\Psi\beta}{\Psi\alpha} \qquad (3.6(b))$$

Now the output Ψm is a DC quantity and the limiter output in strategy 3 is also a DC quantity so in this strategy the same method is used in the magnitude of the output and angle

of the output is controlled normally. The block diagram describing strategy 4 as shown in Figure 9. The results and comparison of strategy 3 and strategy 4 is done in section V.

3.3.5 Algorithm/Strategy 5 (Modified integrator with PI)

In strategy 3 and strategy 4 we have used a limiter. The value of limiter is fixed and should be equal to the reference flux value needed in the AC drives. So, strategy 1 and 2 are used in constant flux AC drives. For the drives with variable flux levels another strategy is introduced. In this the compensation value is not fixed and changed with the flux levels of AC drive. An adaptive approach is implemented which is based the fact that motor flux and motor emf have 90 degree phase between them. Phasor diagram shown in Figure 27 represents the equation 3.4 i.e the total flux is comprises of two parts i.e Ψα and Ψβ, which in turn again comprises of feed forward and feedback components. Now if any component is increased or decreased then the total flux will not have quadrature angle with emf. This results in an error which is given by equation 3.7[7,8].

$$|emf|.\cos\phi = \frac{\phi_{beta}.EMF_{beta}+\phi_{alpha}.EMF_{alpha}}{|\phi|} \qquad (3.7)$$

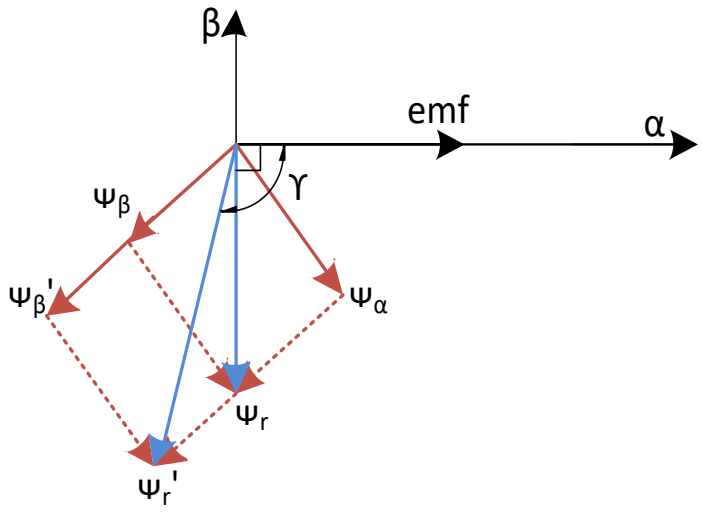

Fig.27. phasor diagram showing relationship between emf and Ψ

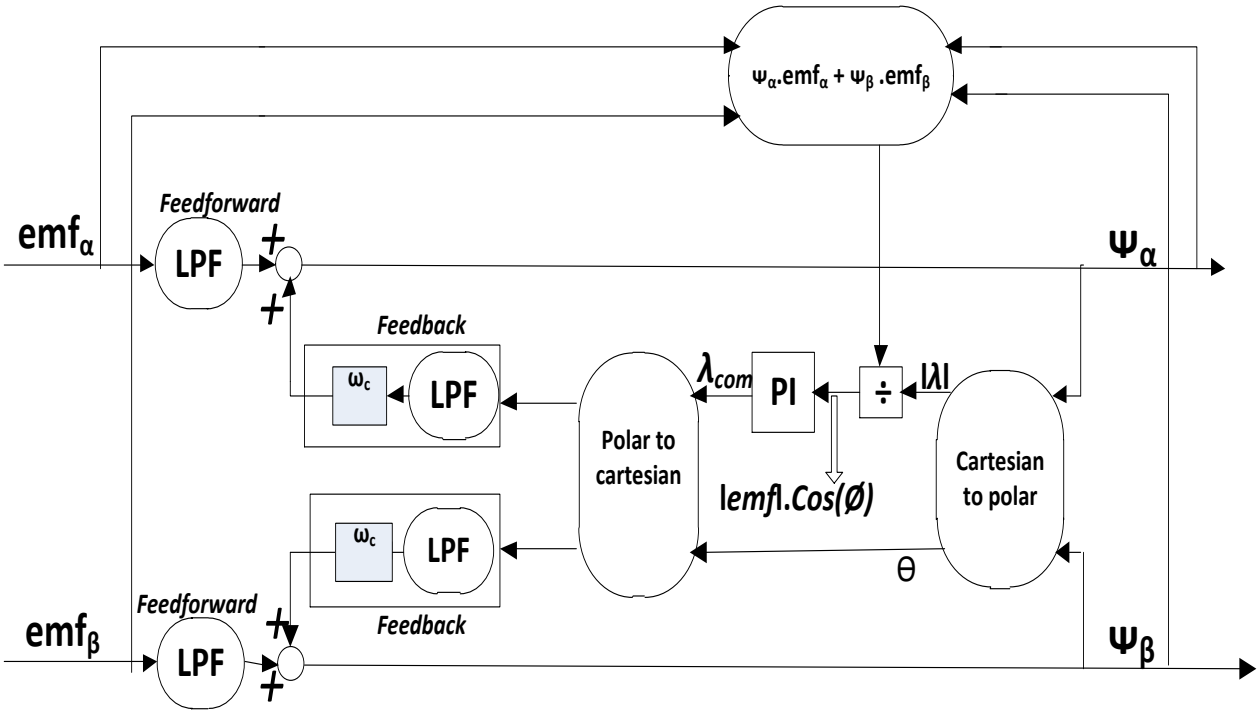

Fig.28. Block diagram for strategy 5

So, a detector is implemented along with PI regulator, Z_{comp} i.e the magnitude component in feedback is calculated from equation 3.8.

$$Z_{\text{comp}} = (k_{\text{p}} + \frac{k_{\text{i}}}{s}).\frac{\phi_{beta}.EMF_{beta} + \phi_{alpha}.EMF_{alpha}}{|\phi|} \quad (3.8)$$

The output of PI regulator will be zero if the angle between emf and the estimated flux is equal to 90 degree. The block diagram describing strategy5 is shown in Figure 28.

3.3.6 Algorithm/Strategy6 (Modified integrator with frequency compensation and cut off frequency tuning)

In all the strategies discussed yet, the cut off frequency of the filters is fixed. An approach is presented in strategy 6. Firstly to compensate the low pass filter errors a simple compensation is provided which is to multiply the LPF block with the inverse of HPF frequency response. The gain and phase of LPF is given in Table 1, and magnitude and phase for inverse of HPF is given in equation 3.9[38,21,8].

$$\frac{\sqrt{(\omega_c{}^2 + \omega_s{}^2)}}{|\omega_s|} \quad (3.9)$$

$$\theta = \tan^{-1}(\frac{\omega_s}{\omega_c}) - \frac{\pi}{2} \quad (3.10)$$

Now the main advantage of this strategy is that the corner frequency of the low pass filter is tuned with respect to the operating frequency of the system. The choice of cut off frequency is very important as a filter which can attenuate the dc offset at high speed may fail to attenuate at low speeds. So, corner frequency is tuned and depends upon the operating frequency as given by equation 3.11.

$$\omega_c = \lambda . |\omega_s| \tag{3.11}$$

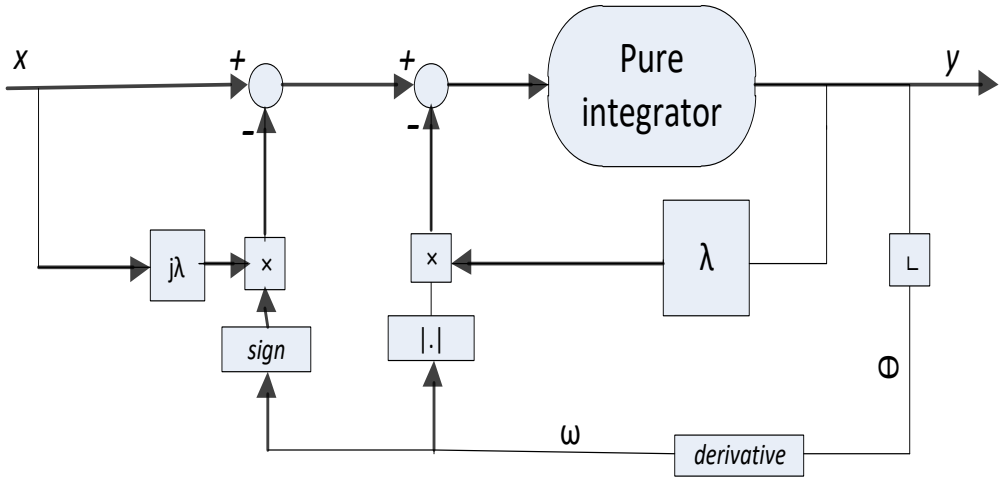

Fig.29. Block diagram for strategy 6

So, the final model of the modified integrator includes a low pass filter block then the compensation of errors given by equation 3.9 and equation 3.10 and then finally the tuning of cut off frequency as given in equation 3.11.

From equations 3.9, 3.10 and 3.11 we can get the modified integrator equation 3.12.

$$y = \int (-\lambda |\omega_s| + [1 - jsign(\omega_s)].x).dt \tag{3.12}$$

where y is the output and x is the input to the modified integrator. Here λ is the designing factor and its value typically lies from 0.1 to 0.5. It should be noticed that for $\lambda = 0$ equation 12 yields pure integrator. The block diagram showing the implementation of equation 12 is shown in fig.29. In this algorithm instead of using the operating frequency from output we can also estimate the operating frequency from the equation 3.13[38,21,8].

$$\omega_s = \frac{[\Psi_{s\alpha}(V_\beta - I_\beta . R_s) - \Psi_{s\beta}(V_\alpha - I_\alpha R_s)]}{[\Psi_\alpha^2 + \Psi_\beta^2]} \tag{3.13}$$

CHAPTER 4

IMPLEMENTATION OF FILTERS ON INDUCTION MOTOR DRIVE

4.1 SIMULATION MODELS

The algorithms discussed in chapter 3 are implemented on the Direct Torque Control model in MATLAB Simulink. The model used for simulink is shown in Figure 30(a) and 30(b).

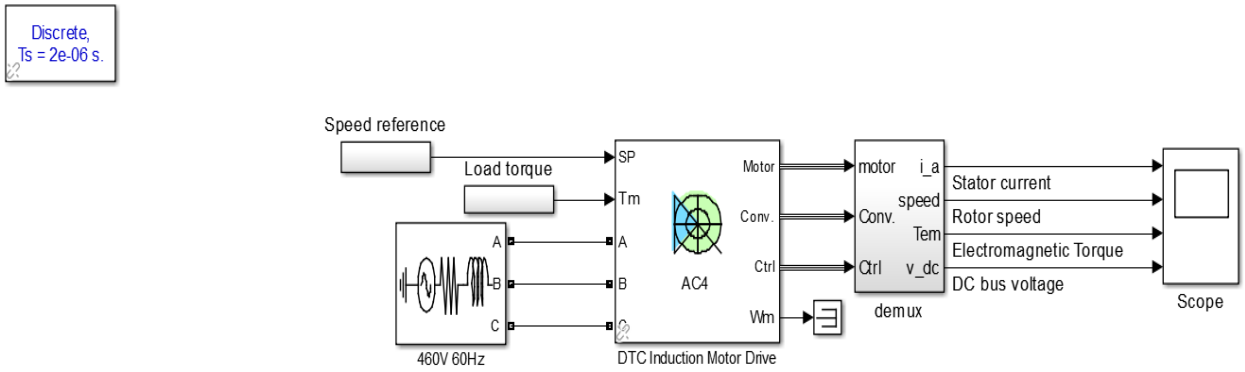

Fig.30(a). Simulation model of Direct Torque Control scheme of Induction Motor (masked)

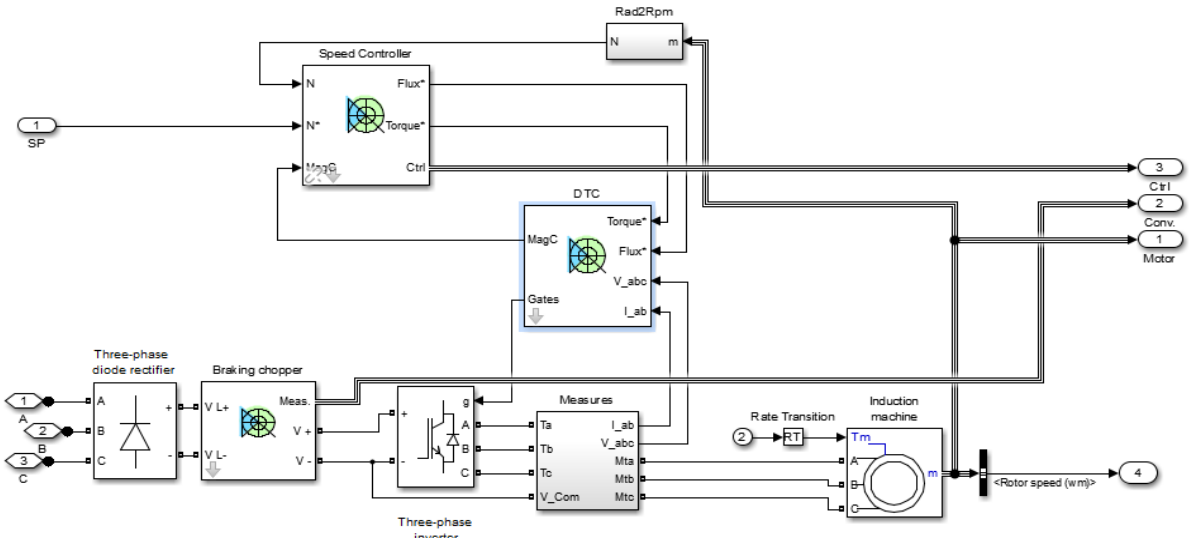

Fig.30(b). Simulation model of DTC scheme of Induction Motor (unmasked).

In Figure 30 (b), the detailed simulation diagram is given, it consist of various components which are described further.

Firstly the 3 phase supply is given to a diode rectifier along with the braking chopper, it is included in the simulation because in real applications the three phase supply is not given directly to the Induction Motor but it goes through two conversions to achieve variable frequency controlling. First stage is AC to DC conversion which is done by rectifiers along with the chopper, then the second conversion which is DC to AC, and it is done by Inverter. In place of using rectifier and braking chopper a simple DC supply can also be given to the Inverter. The main controlling of Induction Motor is through switching pattern of Inverter. The circuit diagram of inverter was described in chapter 1, from which we can see that a three phase inverter has 6 switches, and the switching of these switches decides the controlling of Induction Motor. Now the output of Inverter is directly connected to Induction Motor in build model of MATLAB, the parameters of Induction Motor are given in Table 2.

TABLE II. MOTOR PARAMETERS for DTC DRIVE

Motor parameter	**Value**
Power Rating	149.2 kVA
Number of pole pairs	2
Rated speed	1500 rpm
Stator Self Inductance	0.3027 mH
Rotor Self Inductance	0.3027 mH
Mutual Inductance	10.46 mH
Stator Resistance	14.85 mΩ
Rotor Resistance	9.295 mΩ
Inertia constant	3.1 kgm^2
Friction Coefficient	0.08 Nms

TABLE III. CONTROL PARAMETERS for DTC DRIVE

Control Parameters	Value
Proportional Gain	30
Integral Gain	200
Hysteresis bandwidth Torque	10 Nm
Hysteresis bandwidth flux	0.02 Wb
Initial machine flux	0.8 Wb
Maximum switching frequency	20000 Hz
Sampling time for DTC	$20e^{-6}$ sec

Now as can be seen from Figure 30(b) the output speed of Induction Motor is taken and feed to speed controller block of simulation, the second input to speed controller block is the reference speed, a PI controller is implemented whose input is given as error in speed and the output is taken as Torque reference according to error in speed, so from here the reference torque is generated and also the reference flux is taken as fixed value of 0.8 Wb. The unmasked speed controller block is shown in Figure 31.

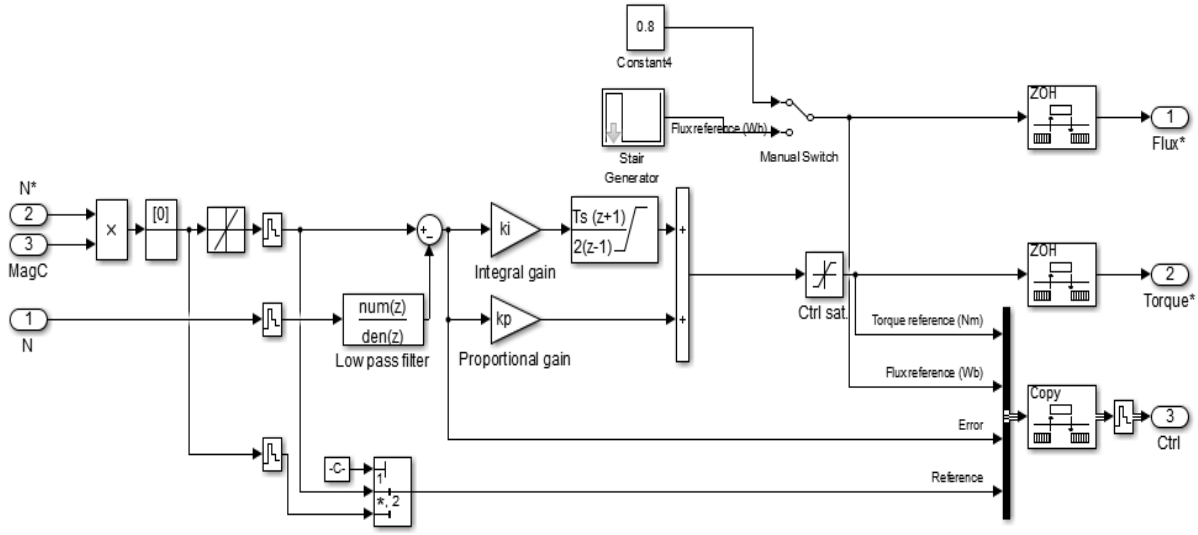

Fig.31. Unmasked speed controller block

Now the output of speed controller i.e the torque reference and the flux reference are fed to the Direct Torque Controller (DTC) scheme. In DTC scheme block two more inputs are needed i.e terminal three phase voltage and current values of Induction Motor. From these values flux is estimated from voltage model of flux estimation and from the estimated flux, torque is estimated[42].

The estimated flux is in two parts i.e d axis flux and q axis flux, the reference is the vector quantity of flux with magnitude and angle as shown in Figure 32.

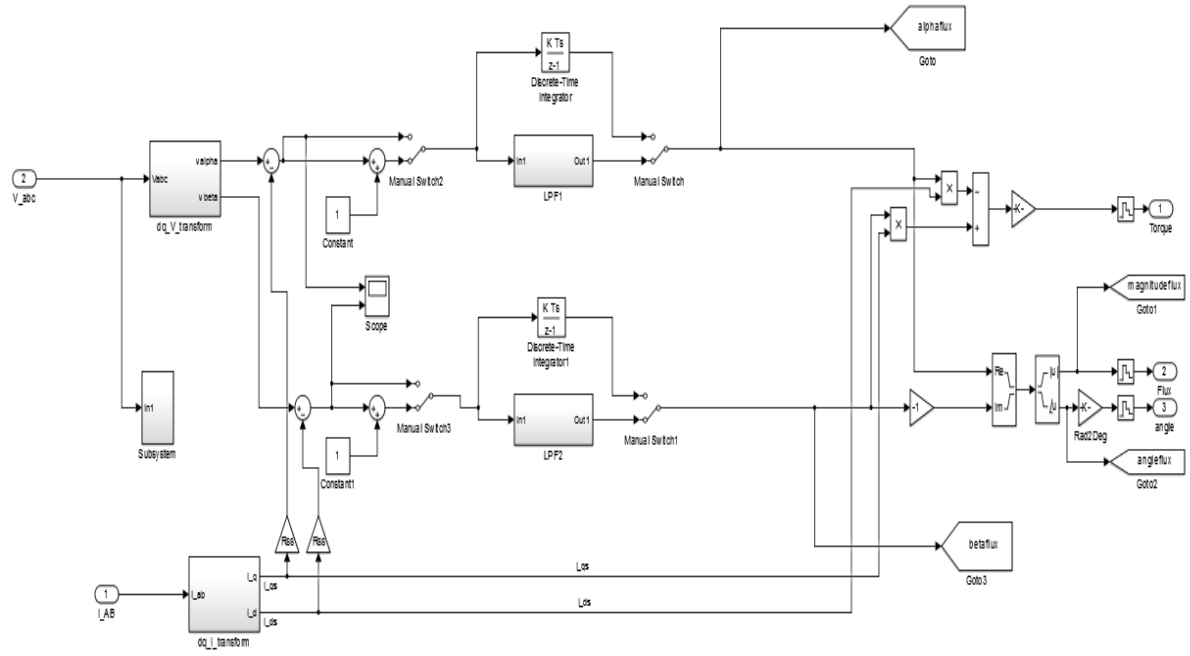

Fig.32. Flux and torque estimation block

Switch is provided for comparison between different algorithms. Now these estimated values are now compared with the reference values and then hysteresis control is provided which gives the output pulses for inverter as shown in Figure 33.

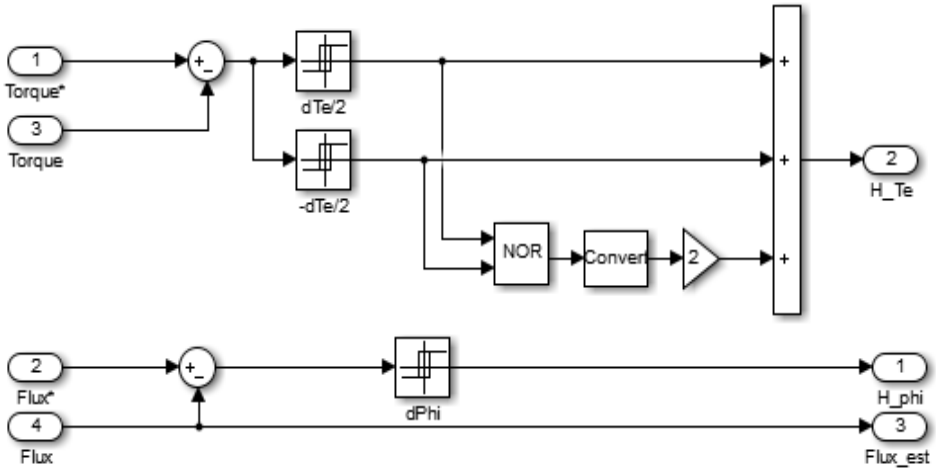

Fig.33. Hysteresis control implemented on torque and flux of IM

4.2. IMPLEMENTATION ON SIMULATION MODEL

Now this model is tested with various algorithms, firstly the original model is tested with a Low pass filter used for voltage model estimation, and speed reference used is 150 rpm and flux reference is motor nominal 0.8 Wb, the results are shown in Figure 34(a) and 34(b).

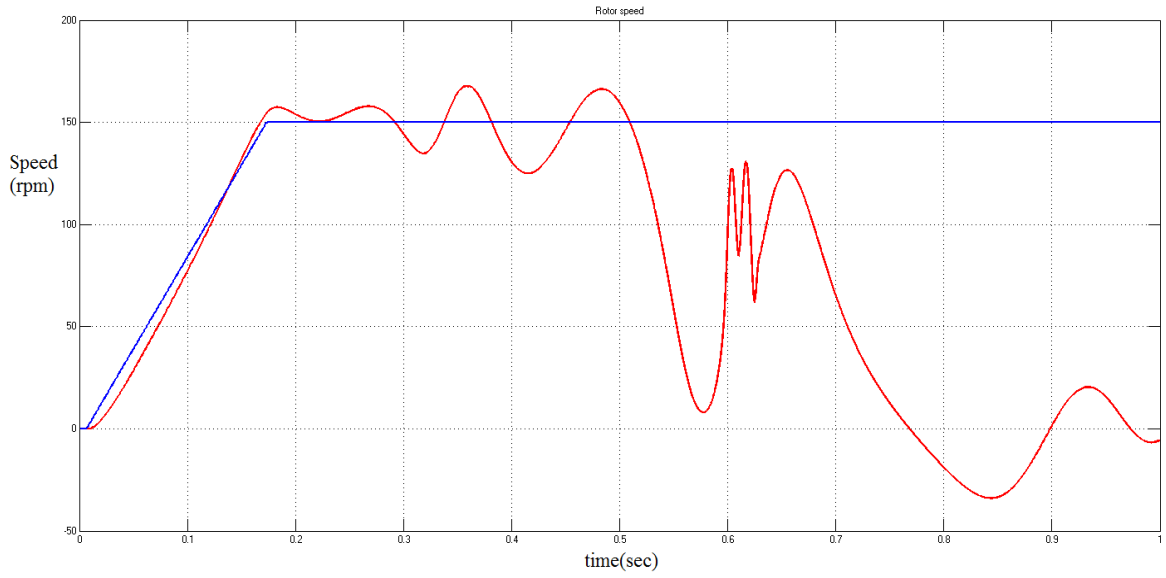

Fig.34(a). Speed response of IM when used with pure integrator with offset

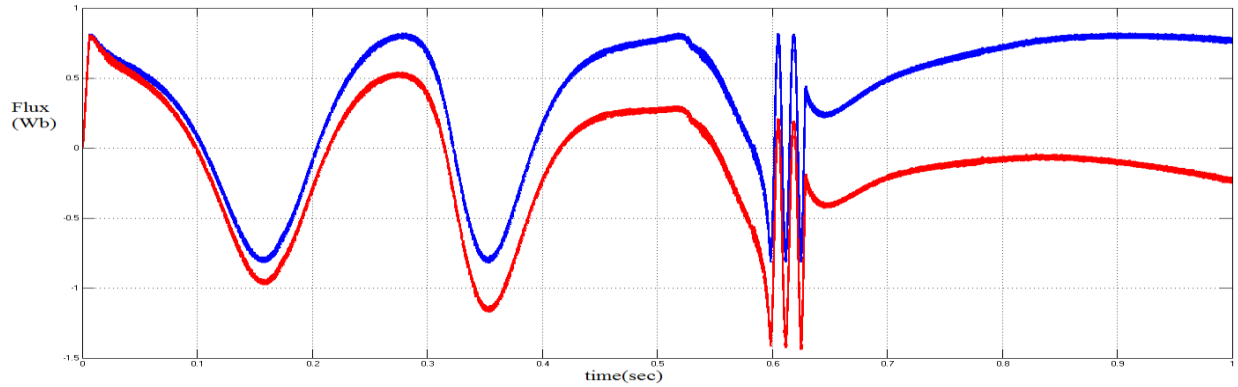

Fig.34(b). Flux estimation of IM when used with pure integrator with offset

With the same operating conditions Low Pass Filter with cut off frequency of 6.28 rad/sec is implemented and the results obtained are shown in Figure 35(a) and 35(b).

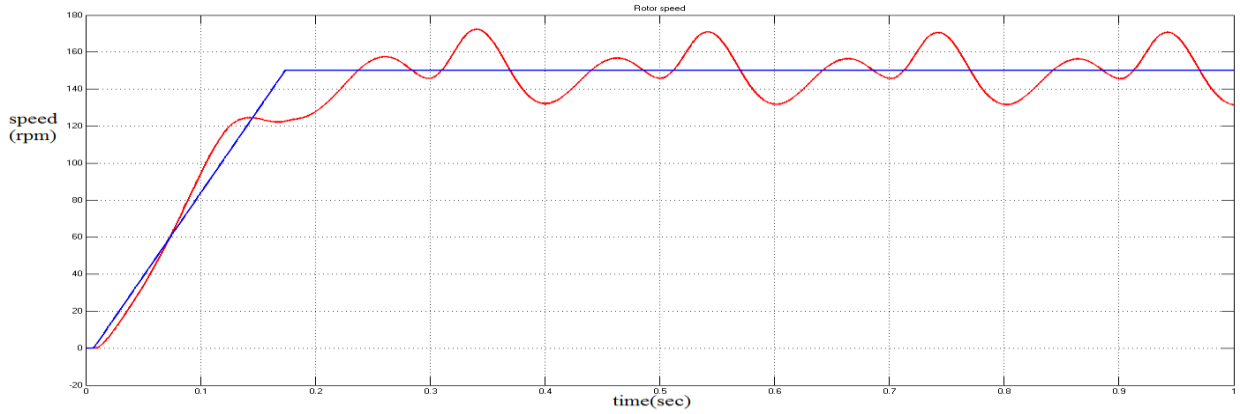

Fig.35(a). Speed response of IM when used with LPF with offset

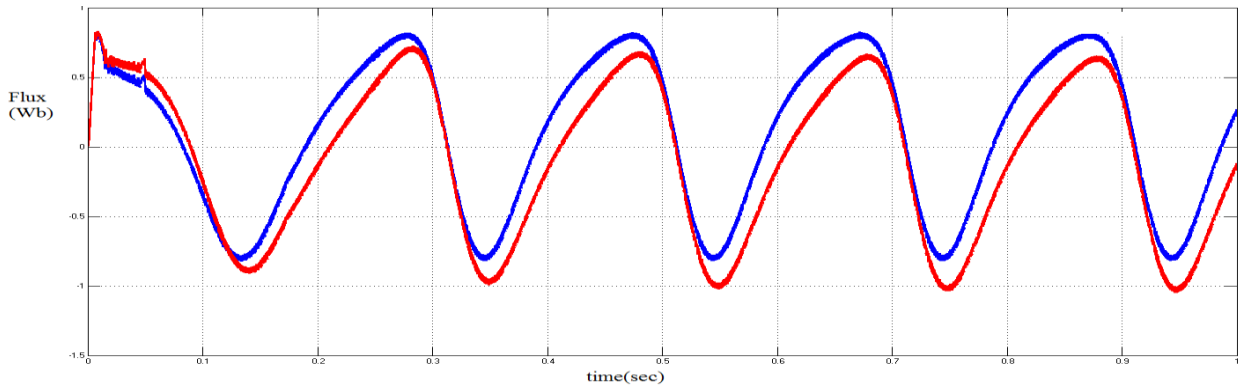

Fig.35(b). Flux estimation of IM when used with LPF with offset

Again with the same operating conditions algorithm 3 is implemented with saturation level set to -0.5 to 0.5 and as expected the predicted flux is less than the actual flux of the machine[41]. The results for this algorithm with this condition are shown in Figure 36(a) and 36(b).

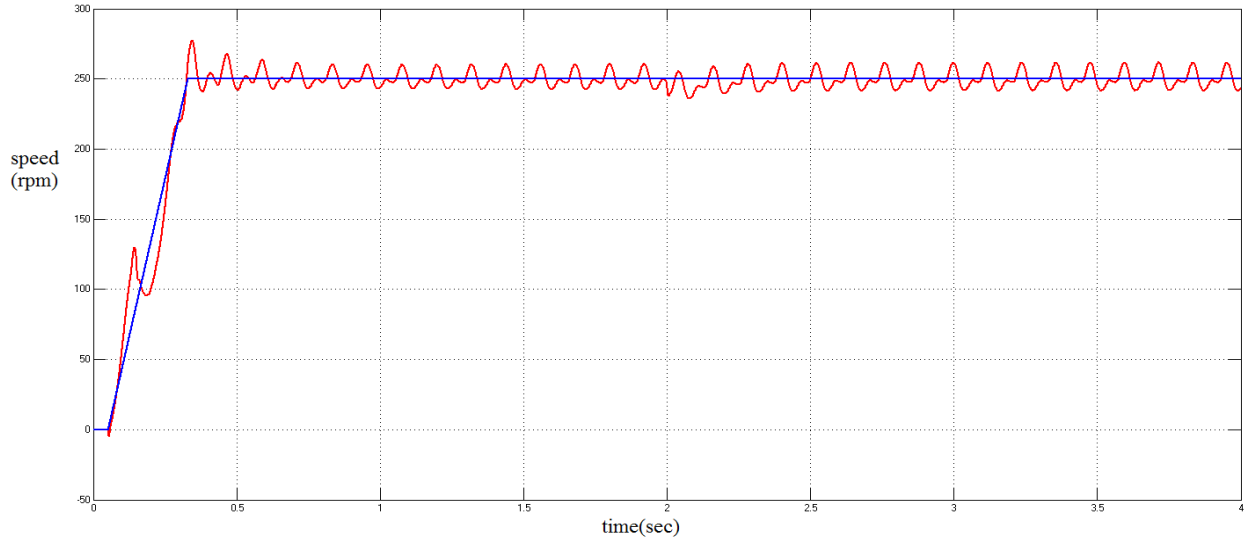

Fig.36(a). Speed response of IM when used with algorithm 3 with saturation -0.5 to 0.5

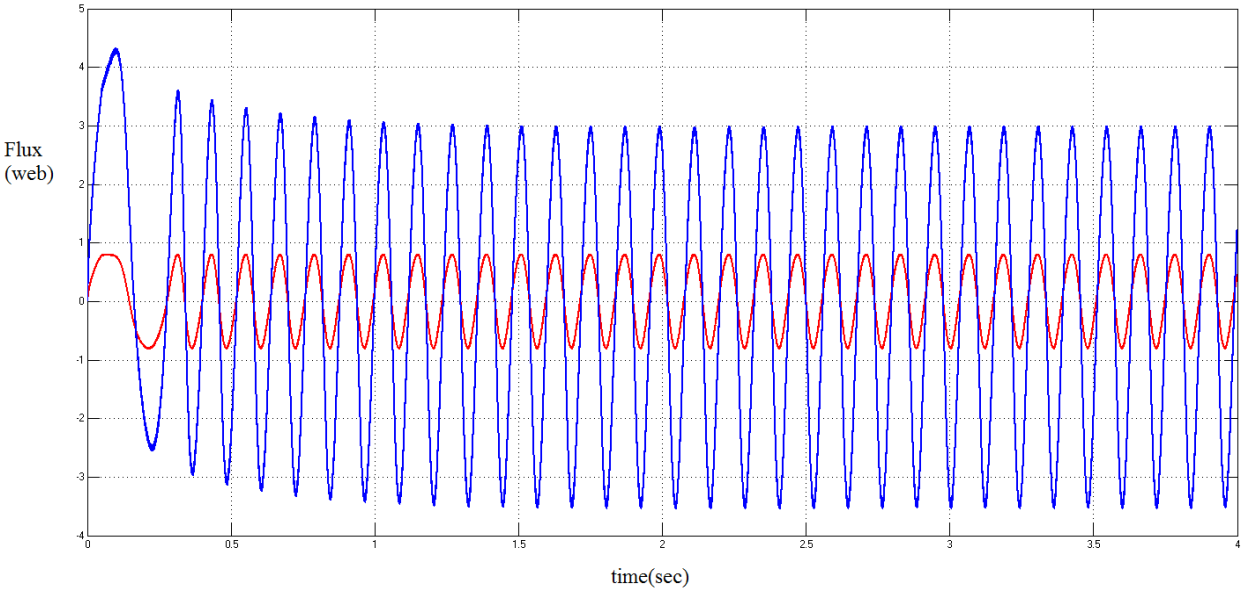

Fig.36(b). Flux estimation of IM when used with algorithm 3 with saturation -0.5 to 0.5

Now with same operating condition but with but if the cut off frequency is increased i.e up to 30rad/sec the results are absurd because by increasing the value of ω_c we are actually increasing the error in the predicted flux.

Now this error in the predicted flux can be controlled and almost eliminated by using the adaptive modified integrator algorithm i.e algorithm 5, the results with proportional gain equal to 0.1 and integral gain equal to 2 and cut off frequency as in the previous case, are shown in Figure 37(a) and 37(b).

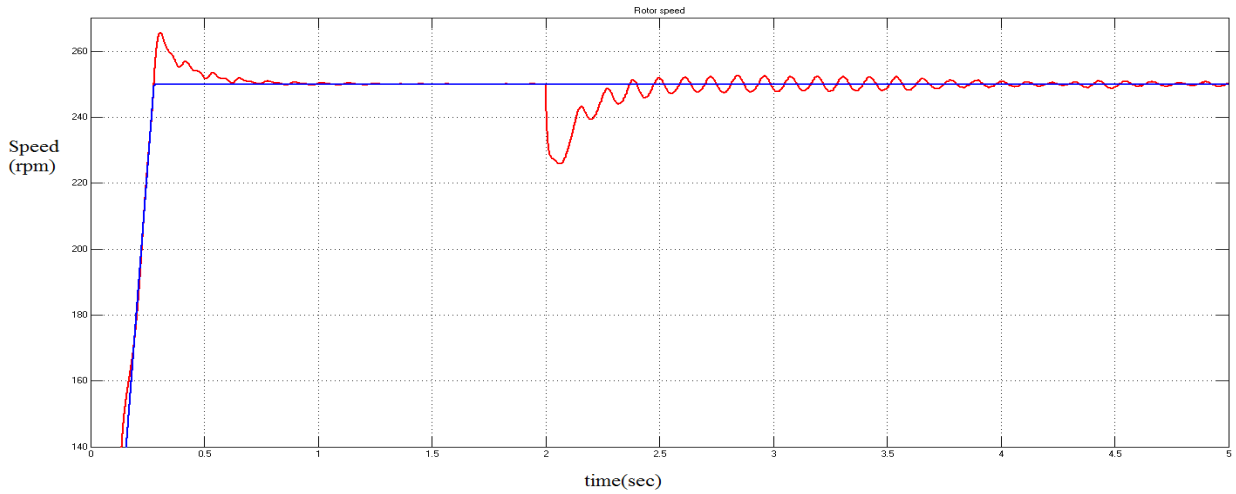

Fig.37(a). Speed response of IM when used with algorithm 5

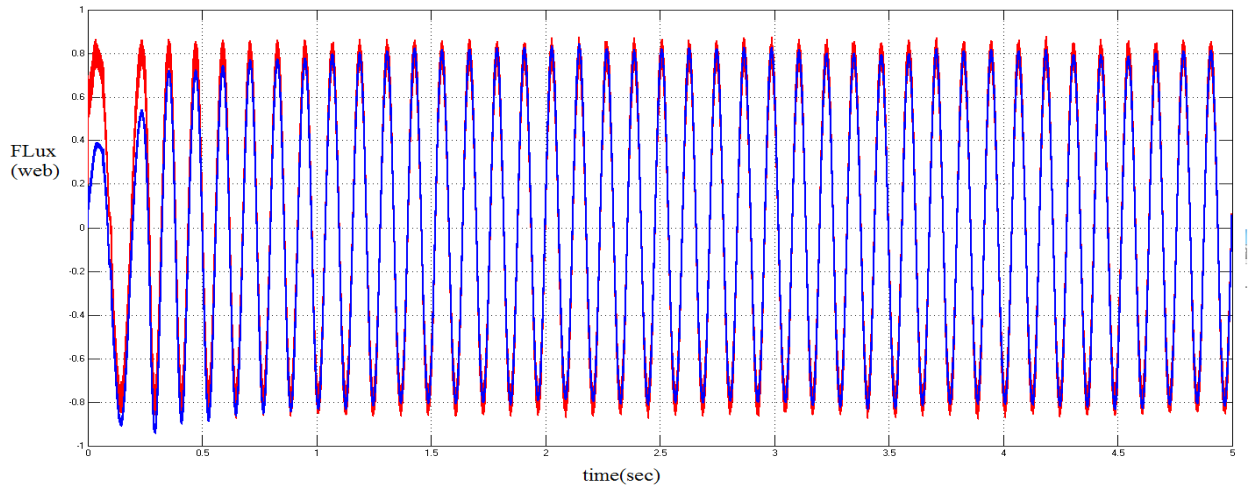

Fig.37(b). Flux estimation of IM when used with algorithm 5

CHAPTER 5

MODEL PREDICTIVE CONTROL

5.1. SIMULATION MODEL FOR DIRECT FOC OF IM

For implementing the predictive control the direct vector control of Induction Motor simulation model is used as shown in Figure 38(a) and 38(b).

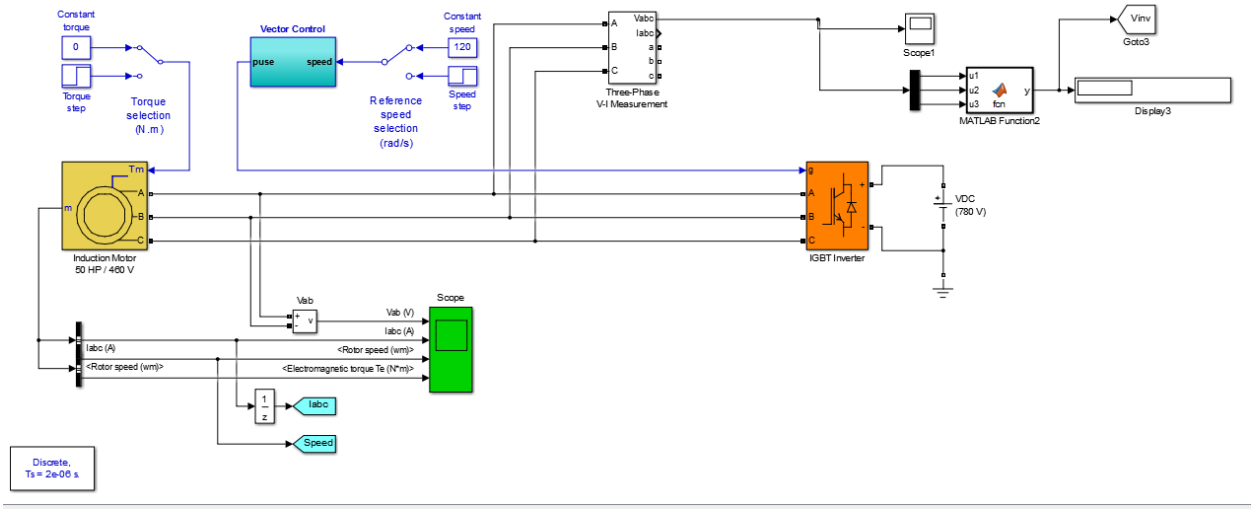

Fig.38(a). Simulation model of Direct Vector Control of Induction Motor (masked)

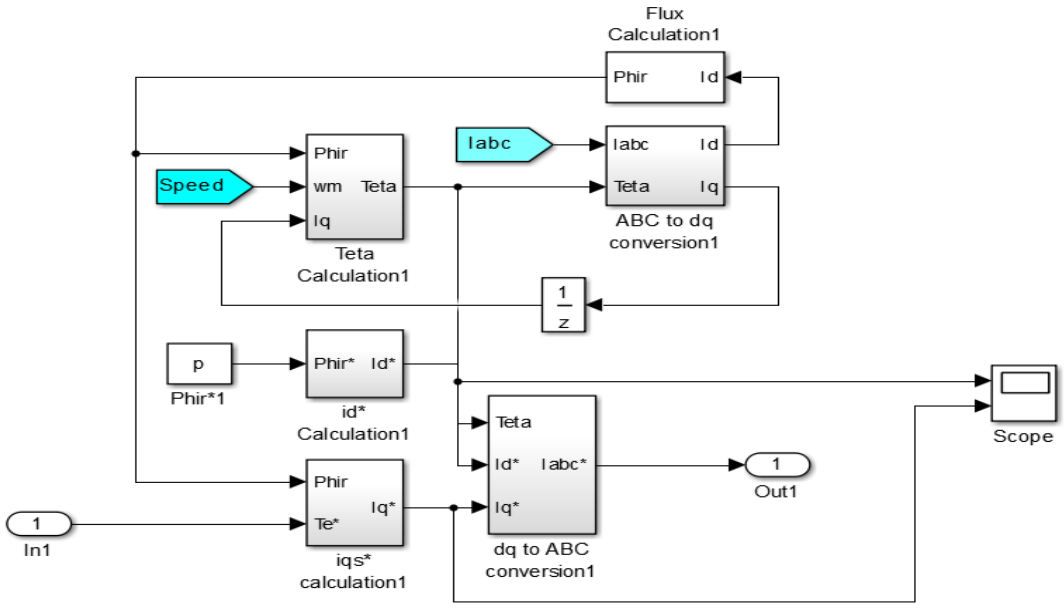

Fig.38(b). Simulation model of Direct Vector Control of Induction Motor (unmasked)

5.2. PREDICTIVE CONTROL

For implementing the predictive algorithm the model used for Induction Motor for forming the equation is used as shown in Figure 39 i.e Induction Motor can be approximated by back emf in series with resistance and inductance for 3 phases[47,48,49].

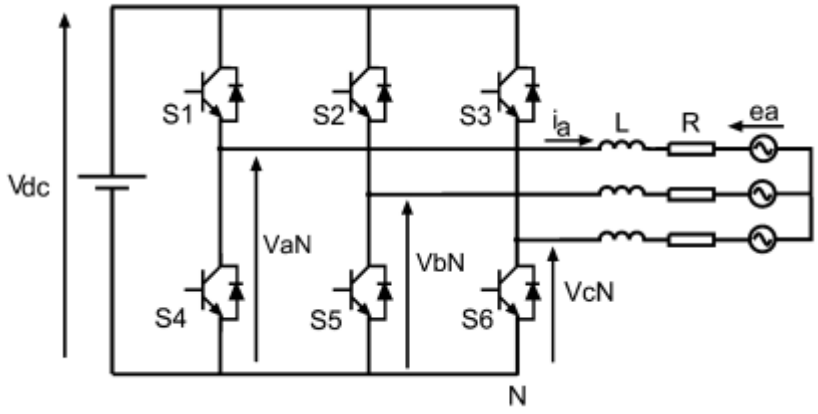

Fig.39. Voltage source inverter with approximated Induction Motor model

From Figure 39 the model equations can be formulated which are given by equations 5.1(a),5.1(b) and 5.2.

$$I = \frac{2}{3}(I_a + a.I_b + a^2.I_c) \qquad (5.1(a))$$

$$e = \frac{2}{3}(e_a + a.e_b + a^2.e_c) \qquad (5.1(b))$$

$$V = R.I + L.\frac{di}{dt} + e \qquad (5.2)$$

Now in Figure 39(b) we have to replace hysteresis current controller by our predictive current controller. Firstly we have to discretize the equation 5.2, and we can write these equations as 5.3 and 5.4.

$$e(k) = v(k) + \frac{L}{T_s}I(k-1) - \frac{R.T_s+L}{T_s}.I(k) \qquad (5.3)$$

$$I(k+1) = \frac{1}{RT_s+1}[l.I(k) + T_s.v(k+1) - T_s.e(k+1) \qquad (5.4)$$

Now from these equations we can find I(k+1), which work as the predicted value of the current and the reference value of current remains the same as in the standard simulation model. In predictive control an objective function is defined and that objective function is subjected to minimize or maximize condition as per the requirement (generally minimize). The objective function used in predictive current control model is given as the sum of absolute errors between the reference and calculated voltages as written in equation 5.5.

$$g = abs\left(real(I_{ref}) - real(I_{meas})\right) + abs(imag(I_{ref}) - imag(I_{meas})) \qquad (5.5)$$

The working of this controller is started by calculating the back emf corresponding to the previous values as given by equation 5.3. Now this back emf is used to calculate the values of predicted current I*, the predicted current I* is calculated correspond to the 8 voltage vectors, i.e I* is calculated with the same value of back emf and other parameters in equation 5.4 and the only vector is voltage vector given by equation 5.6.

$$V = [0; (2/3) * Vdc; (Vdc/3) * (1 + 1.73i); (-Vdc/3) * (1 - 1.73i); -(2/3) * Vdc; (-Vdc/3) * (1 + 1.73i); (Vdc/3) * (1 - 1.73i); 0] \qquad (5.6)$$

So corresponding to this voltage vector of 8elements, 8 values of predicted current will be calculated and then, in the next step the objective function is calculated which is given by equation 5.5, so 8 values of objective function are calculated and actually 7 values of objective functions are calculated because the first and the last element in the voltage vector is zero which gives the same value. Now in the last step the least value of the objective function is chosen and the voltage vector corresponding to which this least value of objective

function occurs is given to the switching of Induction Motor. The subsystems describing the simulation and coding for predictive current control is shown in Figure 40(a),

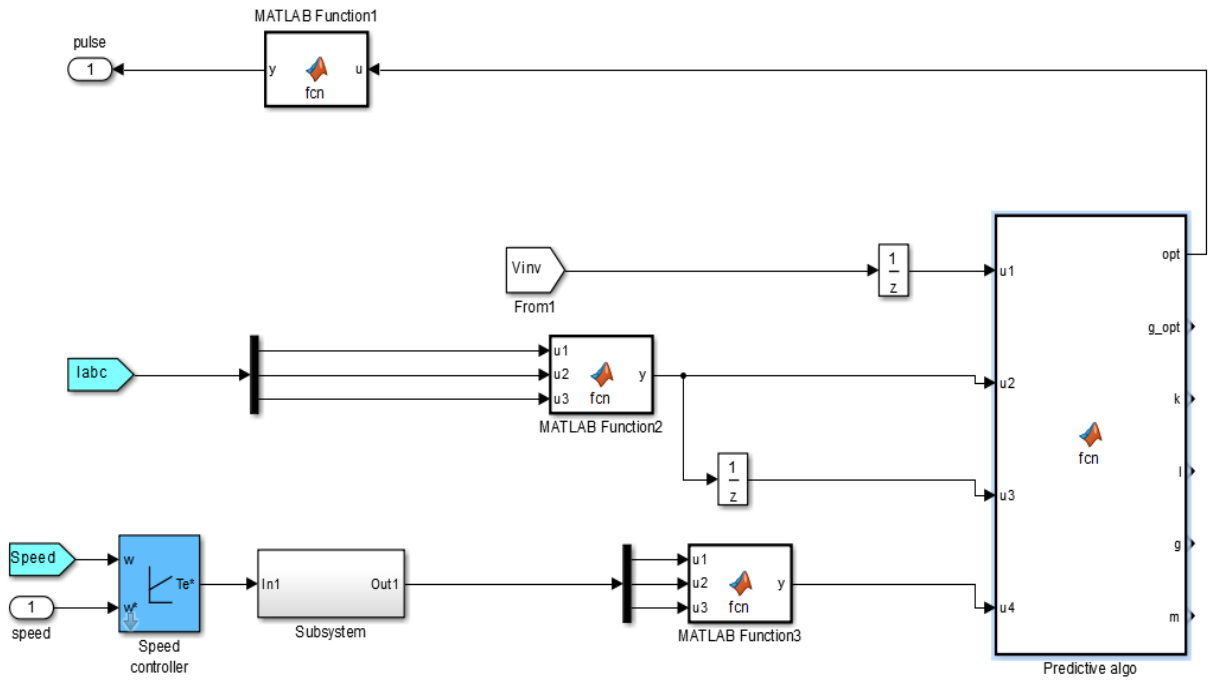

Fig.40(a). Simulation model of predictive algorithm

The MATLAB function 2 and function 3 have the code shown in Figure 40(b).

Vector Control/Predictive algo | Vector Control/MATLAB Function2*

```
1   function y = fcn(u1,u2,u3)
2   %#codegen
3 -  a= cos((2*pi)/3)+((1*i)*sin((2*pi)/3));
4 -  y = (2/3)*(u1+(a*u2)+((a^2)*u3));
```

Fig.40(b). Code to convert 3 phase quantity into vector as in equations 3.1

The MATLAB function namely Predictive Algorithm have the code shown in Figure 40(c) and the switching correspond to optimum switching is decided by MATLAB function 1 block and the code is given in Figure 40(d).

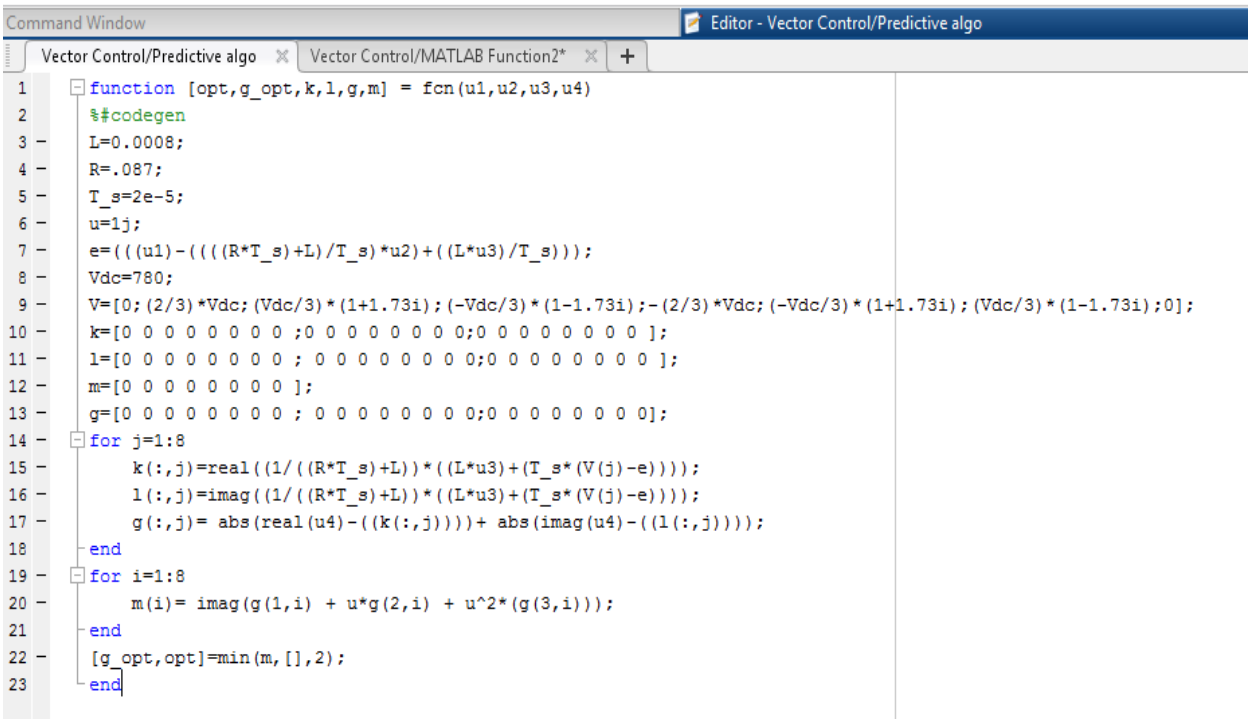

Fig.40(c). Predictive control code used to generate optimum switching for inverter

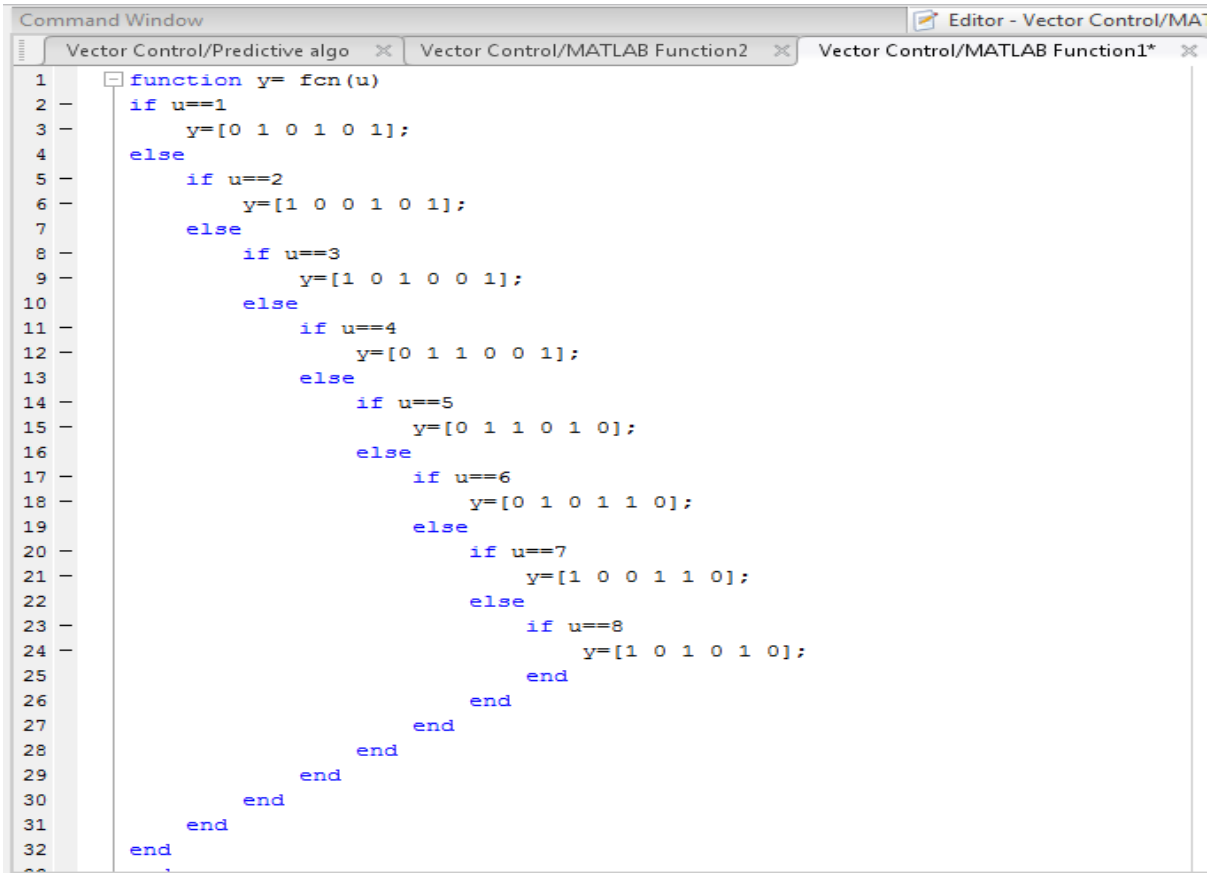

Fig.40(d). Switching pattern of six switches in the inverter code

5.3 RESULTS FOR MODEL PREDICTIVE CURRENT CONTROL ON INDUCTION MOTOR

The results which are the switching pattern of inverter and the speed and torque characteristics of Induction Motor are shown in Figure 41(a) and 41(b).

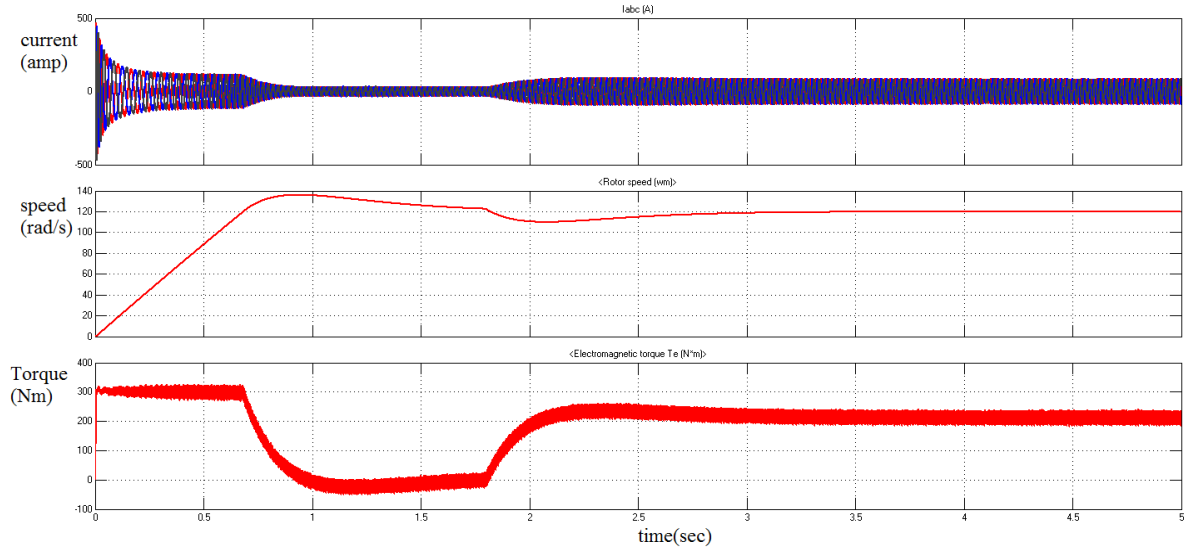

Fig.41(a). Stator current, Speed and Torque characteristics with MPC control with load applied at 1.8 second

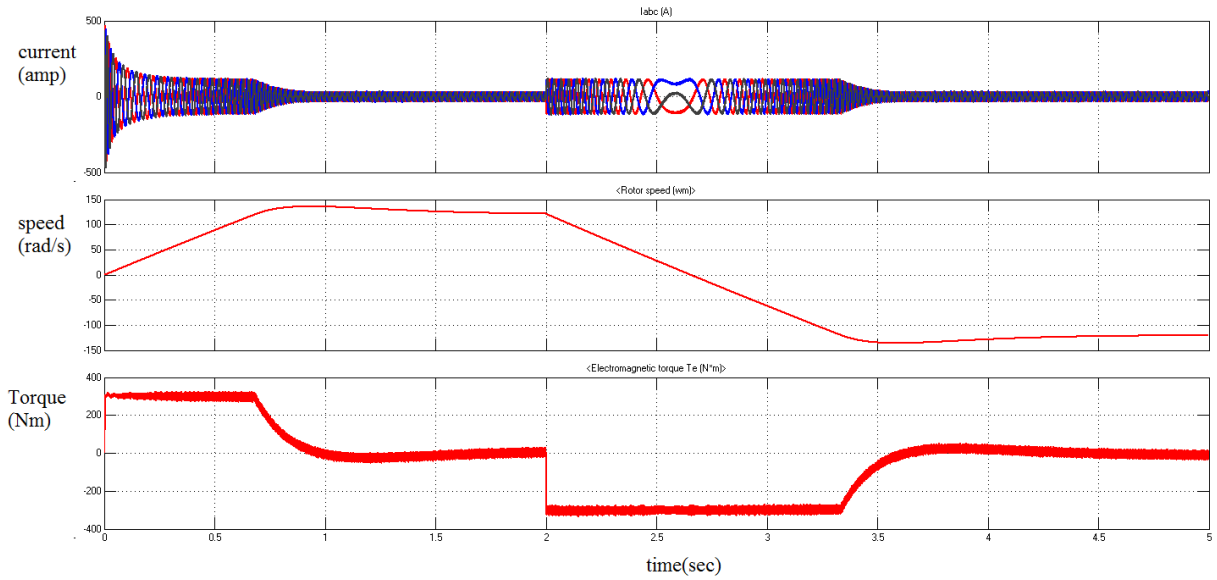

Fig.41(b). Stator current, Speed and Torque characteristics with MPC control with speed reversal

Now it can be seen from the results that the predictive control algorithm is successfully implemented and tested, with loading and also with speed reversal. The motor parameters that are used in simulation are given in Table 4.

TABLE IV. MOTOR PARAMETERS USED FOR SIMULATION of FOC

Motor parameter	**Value**
Power Rating	37.3 kVA
Number of pole pairs	2
Rated speed	1500 rpm
Stator Self Inductance	0.8 mH
Rotor Self Inductance	0.8 mH
Mutual Inductance	34.7 mH
Stator Resistance	0.087 Ω
Rotor Resistance	0.228 Ω
Inertia constant	1.662 kgm^2
Friction Coefficient	0.1 Nms

CHAPTER 6

RESULTS

6.1 RESULTS AND DISCUSSIONS

Every algorithm is implemented and tested with a sinusoidal input. The outputs of the algorithms are then compared with each other.

Fig.42 shows the output of algorithm 1 when a sinusoidal input is given of amplitude 1 pu along with a offset of 0.2 pu and of 1 rad/sec. As shown in Figure 18(b), the integrator is saturated, but by applying algorithm 1 the input is not getting saturated but their exist the initial value problem i.e the output is not lying between -1 to 1 but from -0.5 to 0.9, this introduces the magnitude error. Also the output of a sinusoidal input must be a cosine quantity, which means the output must be 90 degrees apart from the input but as it can be seen from Figure 42 the output is not exactly 90 degrees apart from the input, this introduces phase error.

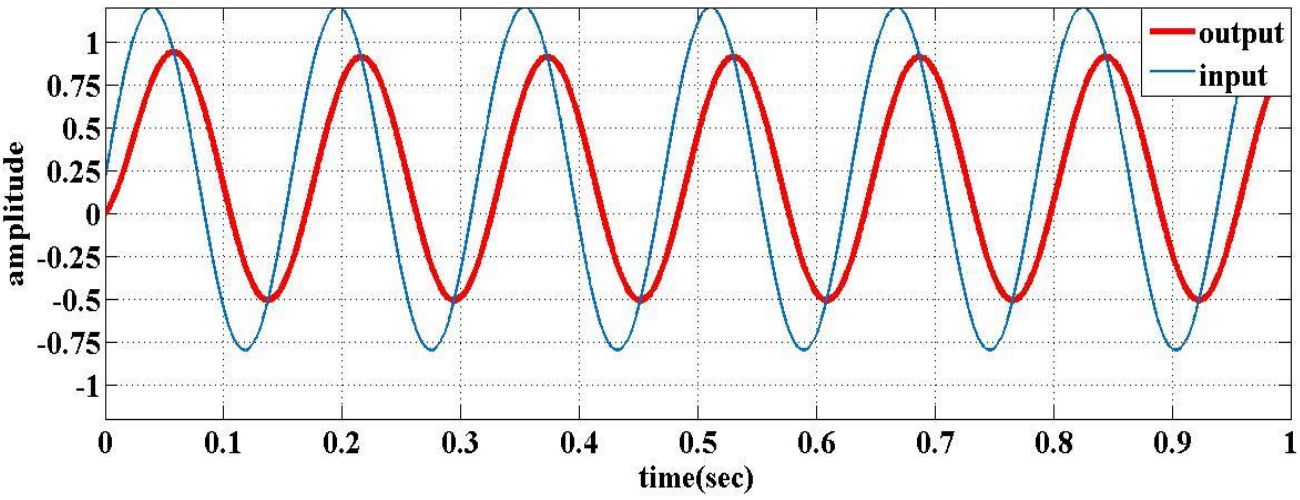

Fig.42. Output of algorithm 1 with sinusoidal input of 1 rad/sec

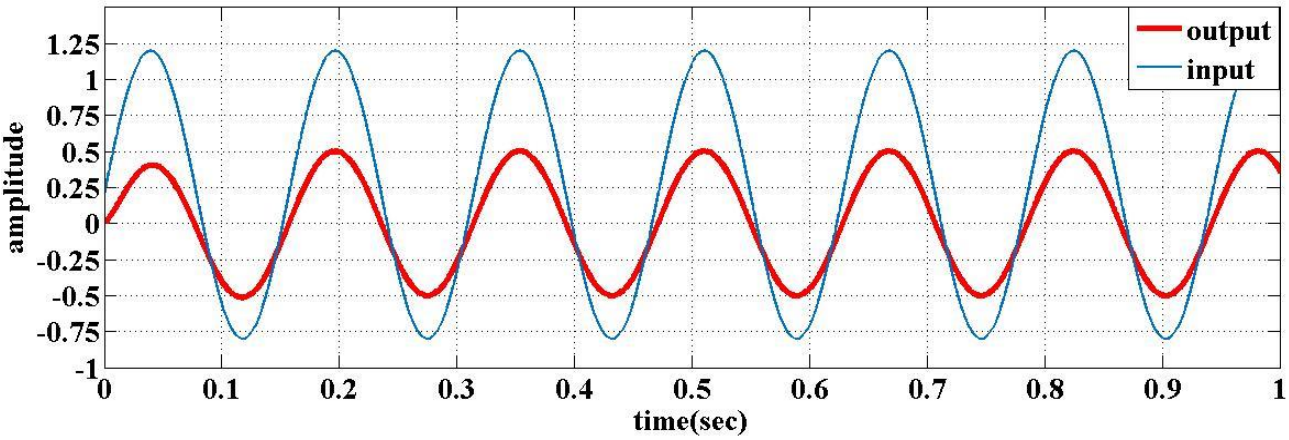

Fig.43. Output of algorithm 2 with sinusoidal input of 1 rad/sec

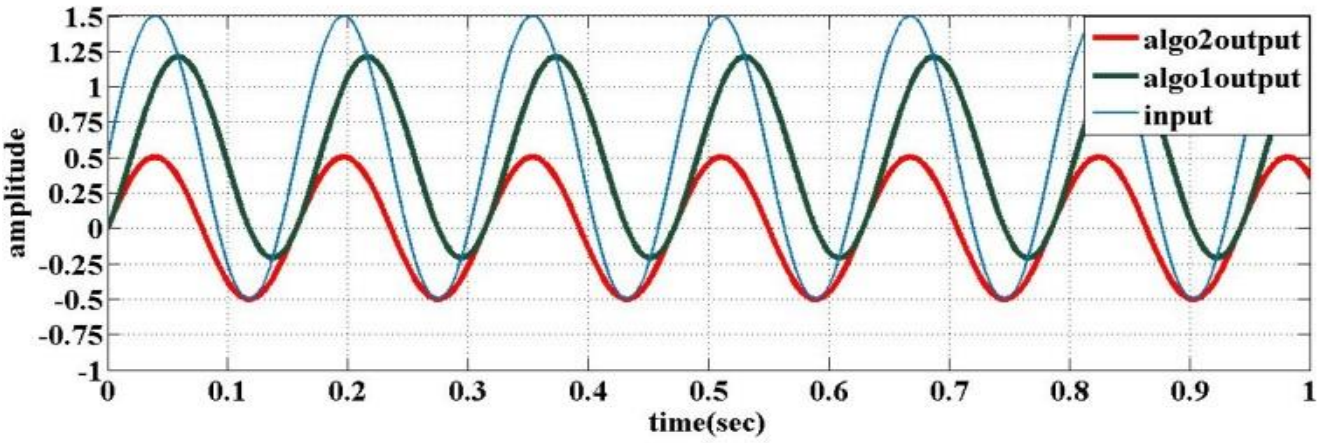

Fig.44. Output of algorithm 1 and 2 with sinusoidal input of 1 rad/sec

Now algorithm 1 is for the low measurement offset errors Figure 43 shows the result of algorithm 2 for same input and Figures 44 shows the comparison of first and second algorithm with the high measurement offset error at input i.e 0.5 pu. As it can be seen from Figure 44 as the offset at the input increases the magnitude error increases in the result of algorithm 1 but in the results of algorithm 2 the magnitude error remains the same as in the previous case, this is because a Low Pass Filter is implemented for compensation.

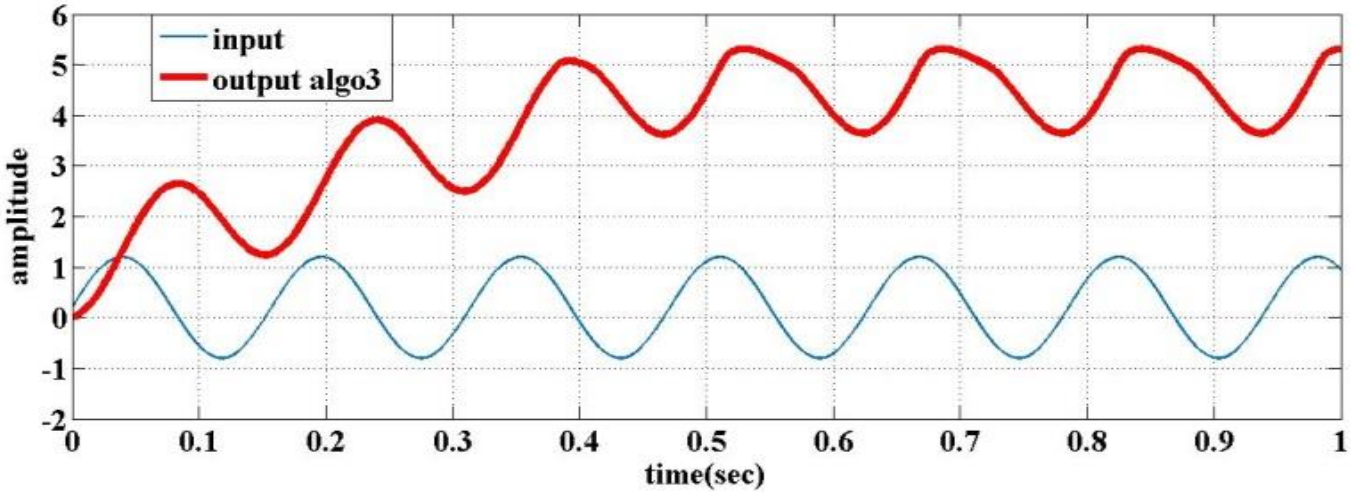

Fig.45(a). Output of algorithm 3 with saturation value (-5 to 5)

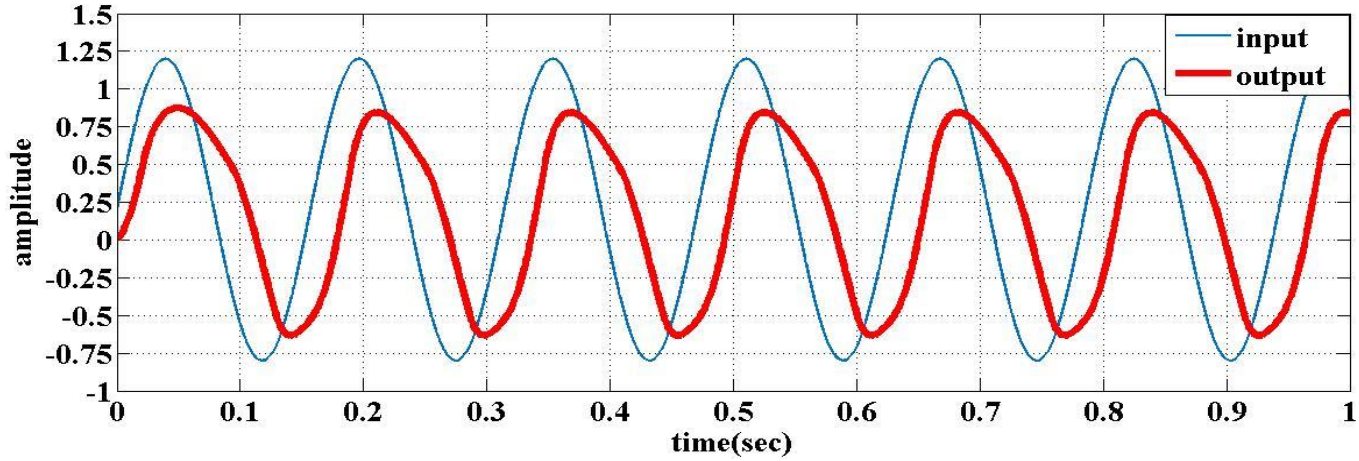

Fig.45(b). Output of algorithm 3 with saturation value (-0.5 to 0.5) pu

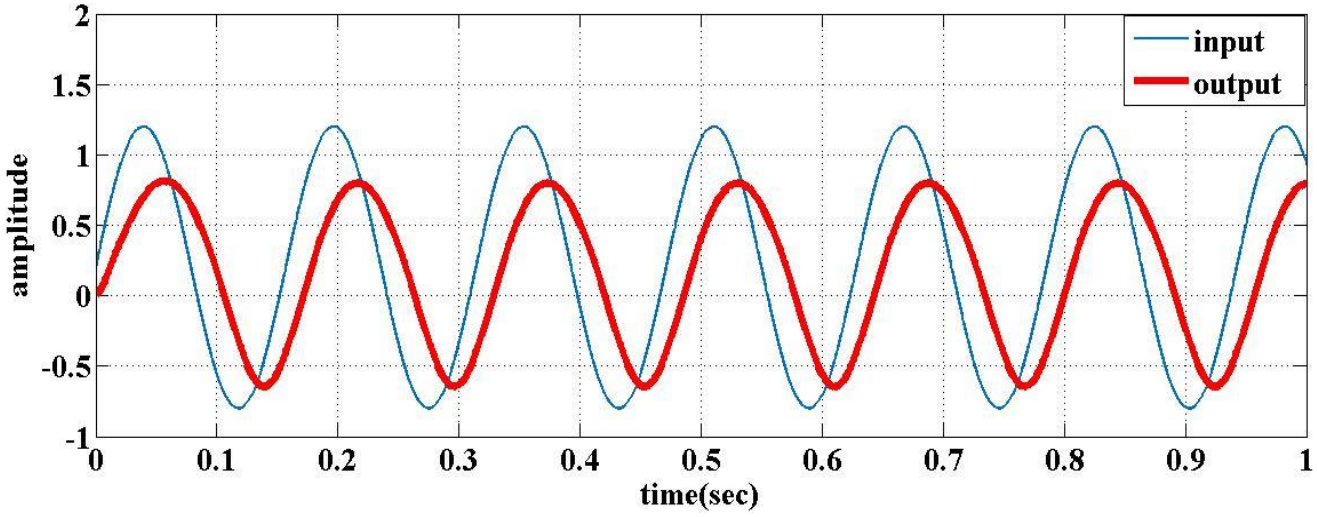

Fig.46(a). Output of algorithm 4 with limiting value 0.5 pu

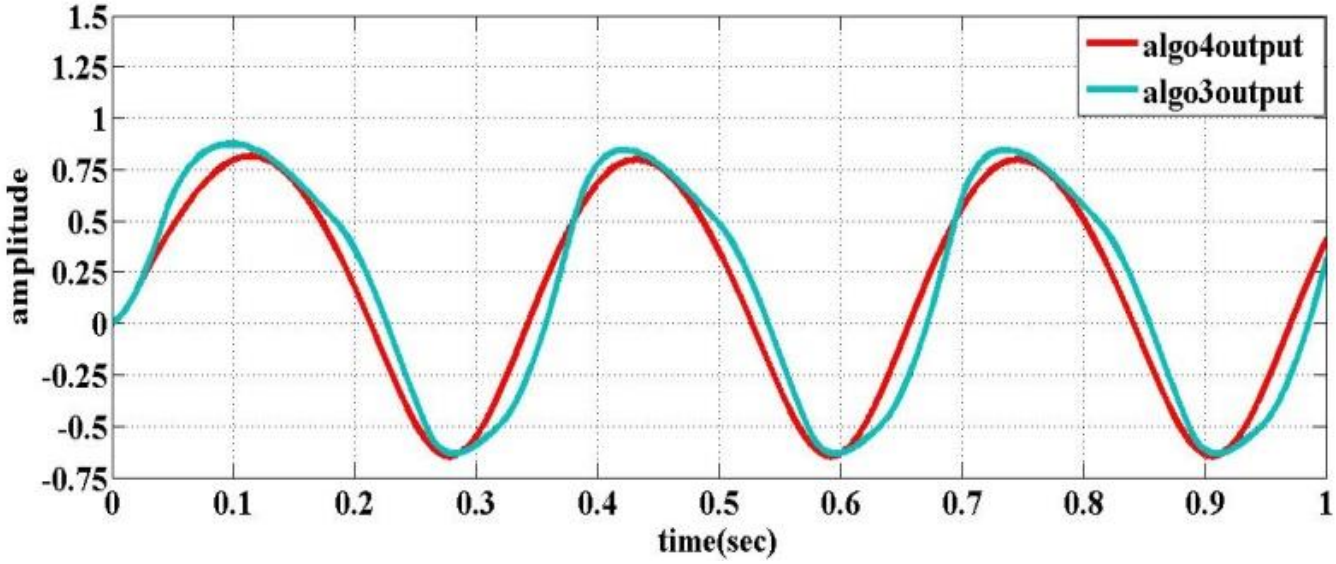

Fig.46(b). Output of algorithm 3 and 4 for same input

The output for algorithm 3 is tested for two values of saturation, Figure 45(a) shows the output when saturation value is set above the reference value i.e -5 to 5, then the output will increase until it reach the upper or lower saturation value, so it consist of a dc offset and Figure 45(b) shows the output when saturation value is set below reference value i.e (-0.5 to 0.5), which results in distortion of the resultant waveform.

To remove this distortion in output waveform another approach is introduced in which the limiting value is set to the magnitude part of the output. Figure 46(a) shows the output for algorithm 4 for similar input, and Figure 46(b) compare the outputs of algorithm 3 and 4.

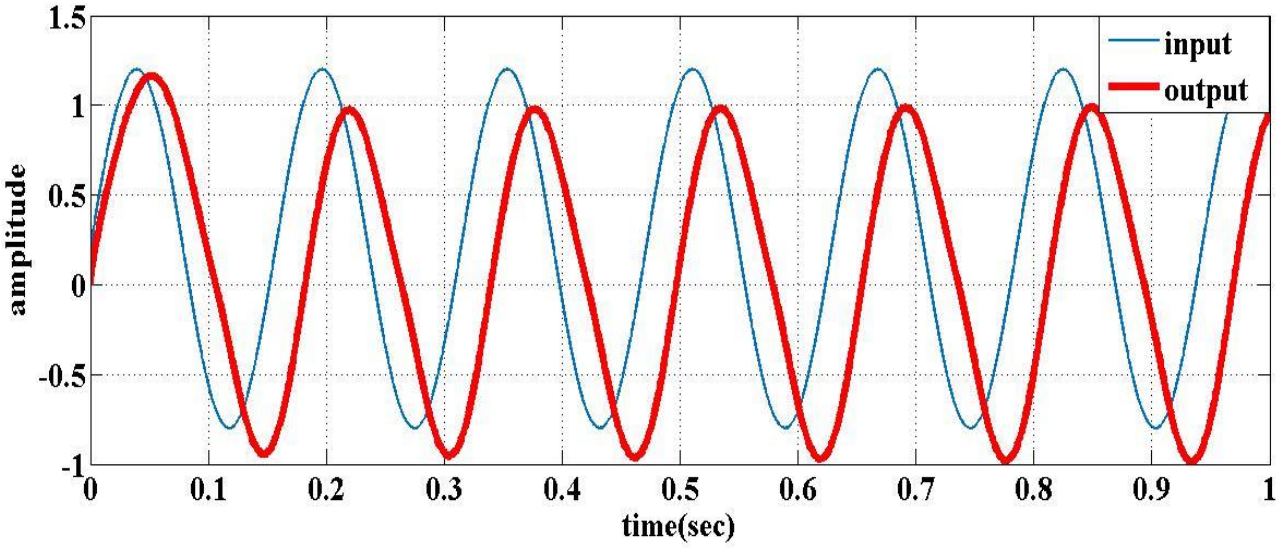

Fig.47. Output of algorithm 5

Now it can be seen from above results that there still exist a phase and magnitude error although the output from last algorithm is acceptable, but it can be used only in the drives where constant flux is needed. For variable flux drive an adaptable approach is needed which is given by algorithm 5.

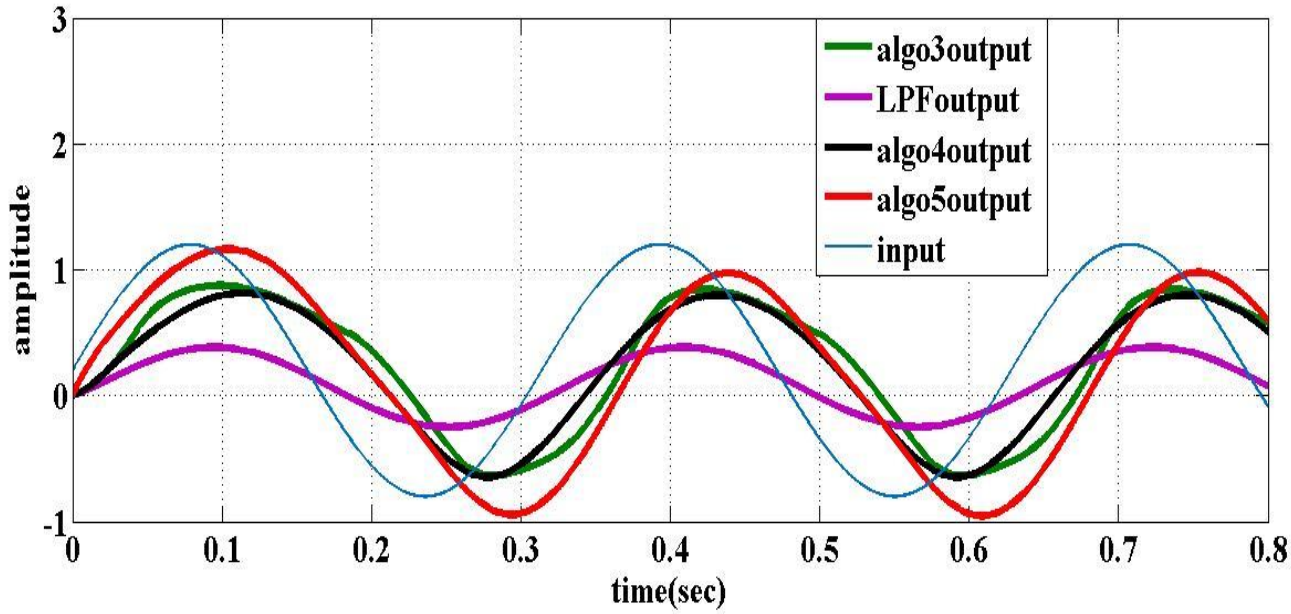

Fig.48. Comparison of output of LPF,algorithm 3,4 and 5

The results for algorithm 5 are shown in Figure 47 with the same input and with the offset of 0.2 pu. It can be seen from the result that the adaptable algorithm gives the best result and the minimum magnitude and phase error. As expected the output for the integration of a sinusoidal input must be a cosine wave with same magnitude because frequency given is 1 rad/sec and the phase between input and output must be 90 degrees. In Figure 47 it is shown that the output is lying between -1 to 1 and phase angle error is also compensated. The comparison between the outputs of all the above algorithms along with the low pass filter output is shown in Figure 48. It can be seen from Figure 48 that with the low pass filter implementation there is large amount of magnitude and phase error, this error is then reduced by applying algorithm 3 but the resultant waveform is distorted, so with the help of algorithm 4 this output is not distorted but still possess a noticeable amount of phase and magnitude error and finally with the implementation of algorithm5 the magnitude and phase errors are compensated.

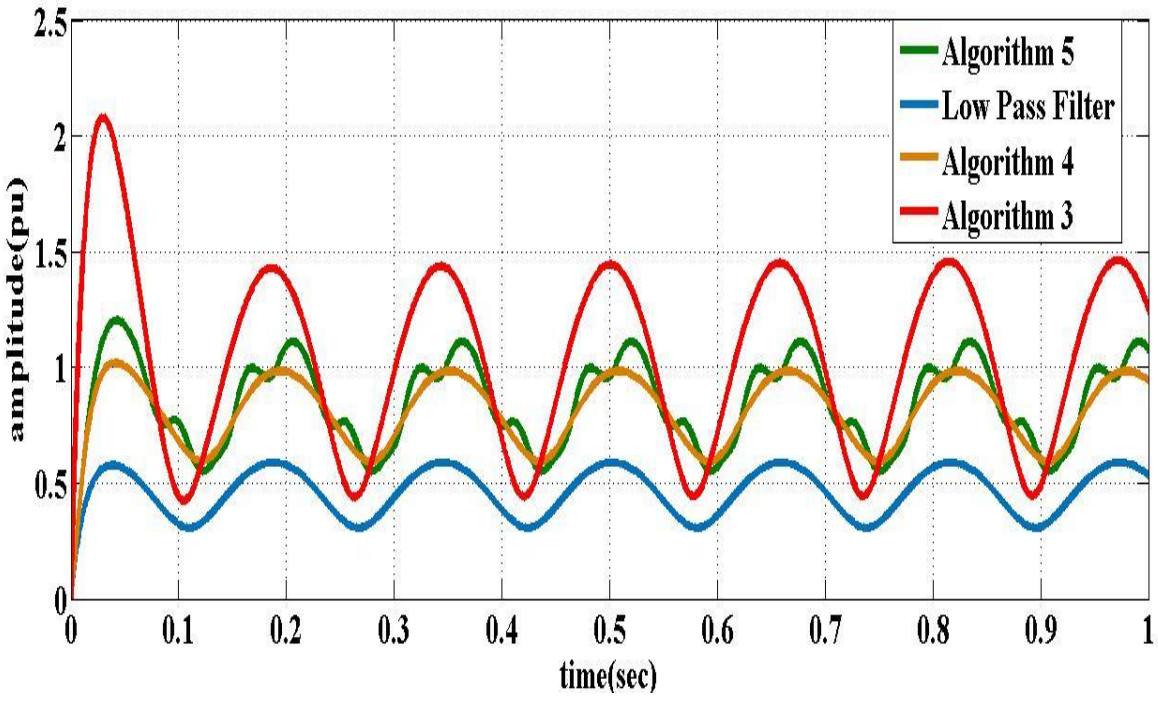

Fig.49. Magnitude response of LPF, algorithm 3,algorithm 4 and algorithm 5

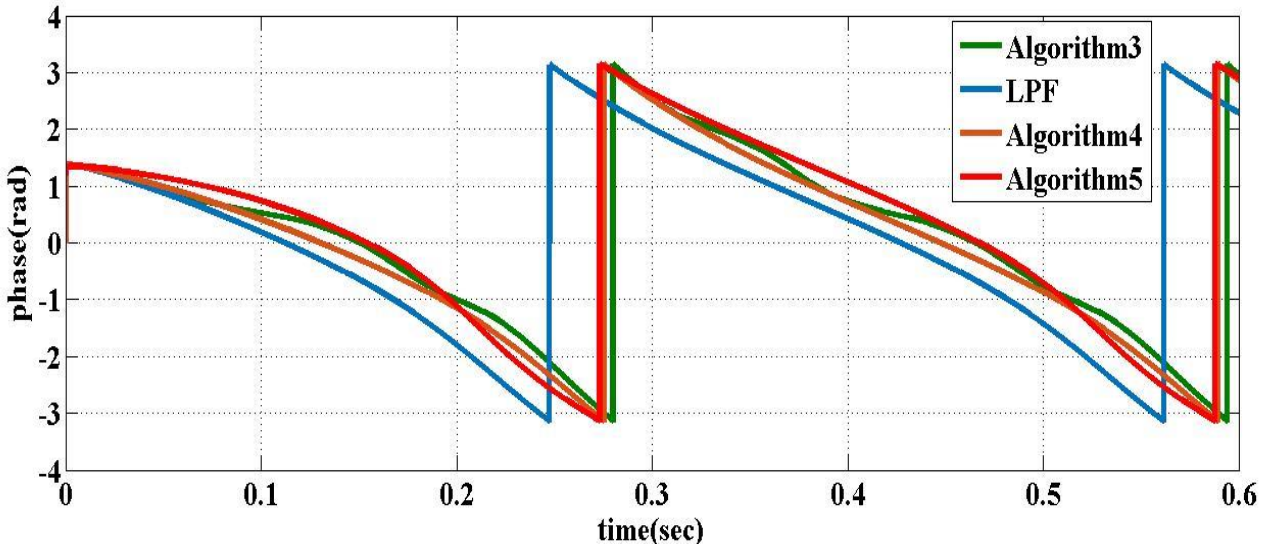

Fig.50. Phase response of LPF, algorithm 3,algorithm 4 and algorithm 5

Figure 49 and Figure 50 shows the magnitude and phase comparison of LPF, algorithm 3, algorithm 4 and algorithm 5. From Figure 49 we can see that low pass filter results gives a huge magnitude error, the result of algorithm 3 is better but have the distorted waveform which is eliminated in the result of algorithm 4, and from Figure 50 also the highest phase error is given by LPF, then algorithm 3 compensate this error but is distorted which is compensated by algorithm 4 and finally the best result is obtained by algorithm 5.

CHAPTER 7

CONCLUSION AND FUTURE SCOPE

7.1. CONCLUSION

In Vector Control of Induction Motor, the most crucial part of the control algorithm is the estimation of rotor flux. To eliminate the problems associate with the pure integration i.e measurement offset problem and initial value problem different algorithms are proposed. All these algorithms are studied and implemented on the Induction Motor drive with Indirect Vector Control and Direct Torque Control. From the analysis of the results it can be concluded that the predicted flux have errors of magnitude and phase when algorithm 1, algorithm 2, algorithm 3 and algorithm 4 is implemented. Algorithm 5 predicts the flux with an adaptive approach along with a PI controller. From the results it can be concluded that the predicted flux follow the measured flux and the controlling is satisfactorily if an offset is provided at the input. The comparative study is done and it can be concluded that the magnitude error is compensated significantly, the phase error persist but the best result for phase compensation comes from Algorithm 5.

The main controlling of Induction Motor is done through the switching of Inverter. Predictive Control is an advanced algorithm which works on the principle of the minimization of an objective function. The predictive current controller concept is studied and implemented on the simulation of Direct Vector Control of Induction Motor. The results are obtained with different running conditions such as with and without load and with speed reversal.

7.2 FUTURE SCOPE

The algorithms discussed in this thesis for better flux estimation can be used in all the drive applications, the work done up till now on these algorithms is on the software platform only with simulink MATLAB. They can be implemented practically on hardware where the saturation problem at low speeds.

Predictive current control is implemented with a objective function which is the absolute difference between the reference and actual current and the results are satisfactory. This concept can be used in minimizing any other objective function, for example an objective function can be decided which gives the losses with the variable parameter of current, the current can be synthesized with the condition that the losses should be minimized and according to that value of current it can be fed to the Induction Motor. Also multi-objective functions can be implemented with this algorithm for better controlling of Induction Motor.

REFERENCES

[1] Nik Rumzi Nik Idris, Member, IEEE, and Abdul Halim Mohamed Yatim, Senior Member, IEEE, "An Improved Stator Flux Estimation in Steady-State Operation for Direct Torque Control of Induction Machines" , IEEE Transactions On Industry Applications, Vol. 38, No. 1, January/February 2002, pp. 110-116

[2] Marko Hinkkanen and Jorma Luomi, "Modified Integrator for Voltage Model Flux Estimation of Induction Motors", IEEE Transactions On Industrial Electronics, Vol. 50, No. 4, August 2003, pp. 818-820

[3] Mohamad Koteich, "Flux estimation algorithms for electric drives: a comparative study", Inter-national Conference on Renewable Energies for Developing countries (REDEC 2016), Jul 2016, Zouk Mosbeh, Lebanon. REDEC 2016.

[4] Jun Hu and Bin Wu, Member, IEEE, "New Integration Algorithms for Estimating Motor Flux over a Wide Speed Range", IEEE Transactions On Power Electronics, Vol. 13, No. 5, September 1998, pp. 969-977.

[5] Kevin D. Hurst, Member, IEEE, Thomas G. Habetler, Senior Member, IEEE, Giovanni Griva, and Francesco Profumo, Senior Member, IEEE, "Zero-Speed Tacholess IM Torque Control: Simply a Matter of Stator Voltage Integration" , IEEE Transactions On Industry Applications, Vol. 34, No. 4, July/August 1998, pp. 790-795

[6] Hao Zhang and Xianzhong Dai, "Stator Flux Oriented Control With Improved Integrator for Speed-Sensorless Induction Motor Drives" , unpublished

[7] Yong Yi, Hailong Song, and Diangui Xu, "Research on Speed Sensorless Vector Control of Induction Motor based on Flux ORientation", IEEE Power Electronics Specialists Conference PESC, 2002.

[8] D. Seyoum, F. Rahman and C. Grantham, "An Improved Flux Estimation in Induction Machine for Control Application", unpublished.

[9] B. Srinu Naik, "Comparison of Direct and Indirect Vector Control of Induction Motor", International Journal of New Technologies in Science and Engineering Vol. 1, Issue. 1, Jan. 2014.

[10] José Rodríguez, Senior Member, IEEE, Jorge Pontt, Senior Member, IEEE, César A. Silva, Member, IEEE,Pablo Correa, Pablo Lezana, Member, IEEE, Patricio Cortés, Student Member, IEEE, and Ulrich Ammann, "Predictive Current Control of a Voltage Source Inverter", IEEE Transactions On Industrial Electronics, Vol. 54, No. 1, February 2007, pp. 495-503.

[11] Rahul Modanwal, S.K.Singh, Pushpender singh, Raj Kumar Sagar, Sanjay Singh, "Hysteresis Vector Controller for Three Phase Induction Motor", International Journal Of Scientific & Technology Research Volume 1, Issue 6, July 2012.

[12] Sergio Vazquez, Jose I. Leon, Leopoldo G. Franquelo, Jose RodrÍguez, Hector A. Young, Abraham Marquez, and Pericle z\Zanchetta, "Model Predictive Control A Review of Its Applications in Power Electronics", IEEE industrial electronics magazine, march 2014.

[13] Yongchang Zhang, Member, IEEE, and Haitao Yang, Student Member, IEEE, "Model-Predictive Flux Control of Induction Motor Drives With Switching Instant Optimization", IEEE Transactions On Energy Conversion, Vol. 30, No. 3, September 2015, pp. 1113-1122.

[14] S. Alireza Davari, "Predictive Direct Angle Control of Induction Motor", IEEE Transactions On Industrial Electronics, Vol. 63, No. 8, August 2016, pp. 5276-5284.

[15] Yongchang Zhang, Member, IEEE, Haitao Yang, and Bo Xia, "Model-Predictive Control of Induction Motor Drives: Torque Control Versus Flux Control", IEEE Transactions On Industry Applications, Vol. 52, No. 5, September/October 2016, pp.4050-4060.

[16] Ass. Prof. Yasser G. Dessouky and Eng. Mona Moussa, "Vector Controlled-Induction Motor Drive: Operation And Analysis", unpublished

[17] B. K. Bose and N. R. Patel, "A programmable cascaded low-pass filter based flux synthesis for a stator flux-oriented vector-controlled induction motor drive," IEEE Trans. Ind. Electron., vol. 44, pp. 140–143, Feb.1997.

[18] J. Holtz and J. Quan, "Sensorless vector control of induction motors at very low speed using a nonlinear inverter model and parameter identification," in Conf. Rec. IEEE-IAS Annu. Meeting, vol. 4, Chicago, IL, Sept./Oct. 2001, pp. 2614–2621.

[19] M. Koteich, G. Duc, A. Maloum, and G. Sandou, "A unified model for low-cost high-performance ac drives: the equivalent flux concept," in The Third International Conference on Electrical, Electronics, Computer Engineering and their Applications (EECEA), Apr. 2016.

[20] I. Takahashi and T. Noguchi, “A new quick response and high efficiency control strategy of an induction motor,” IEEE Trans. Ind. Applicat., vol. 22, no. 5, pp. 820–827, 1986.

[21] X. Xu, R. Doncker, and D. W. Novotny, “A stator flux oriented induction machine drive,” in IEEE PESC Conf. Rec., 1988, pp. 870–876.

[22] H. Tajima and Y. Hori, “Speed sensorless field oriented control of the induction machine,” in IEEE IAS Conf. Rec., 1991, pp. 385–391.

[23] R. Wu and G. R. Slemon, “A permanent magnet motor drive without a shaft sensors,” IEEE Transaction on Industry Applications, Vol. 27, No. 5, 1991, pp. 1005-1011.

[24] Xingi Xu, Rik De Doncker and Donald W. Novotny “A stator flux oriented induction machine drive,” PESC 1988, pp. 870-876.

[25] T. A. Lipo and K. C. Chang, “A new approach to flux and torque sensing in induction machines,” IEEE Trans. Ind. Applicat., vol. IA-22, pp. 731–737, July/Aug. 1986.

[26] P. Tiitinen, P. Pohjalainen, and J. Lalu, “Direct torque control,” Motion Control, pp. 16–19, May/June 1996.

[27] H. Bausch, Z. Wnyan, and K. Kanelis, “Tacholess torque control of induction machines based on the improved voltage flux model,” in Proc. 2nd Chinese Int. Conf. Electric Machines (CICEM), 1995, pp. 180–185.

[28] T. Ohtani, N. Takada, and K. Tanaka, “Vector control of induction motor without shaft encoder,” in Conf. Rec. IEEE-IAS Annu. Meeting, 1989, pp. 500–507.

[29] Jean-Marie Retif, Xuefang Lin-Shi, Florent Morel, “Predictive Current Control for an Induction Motor”, PESC, Jun 2008, Rhodes, Greece. pp.3463-3468, 2008.

[30] G. Victor Raj, K.Venkataramana and V.Chaitanya, “Predictive Vector Control Based Induction Motor Drive using Fuzzy Controller”, International Journal of Science, Engineering and Technology Research (IJSETR), Volume 4, Issue 11, November 2015.

[31] Yongchang Zhang, Member, IEEE, and Haitao Yang, Student Member, IEEE, “Two-Vector-Based Model Predictive Torque Control without Weighting Factors for Induction Motor Drives”, IEEE Transactions On Power Electronics, Vol. 31, No. 2, February 2016, pp. 1381-1390.

[32] Fan, Sheng Wen, Xin Yong Zhao, Zheng Xi Li, and Hu Zhang. "A Flux Observer of VoltageCurrent Model Based on PI Regulator"Advanced Materials Research, 2011.

[33] [Online]. Available: https://en.wikipedia.org/wiki/Model_predictive_control

[34] P.L. Jansen. "A self-tuning, closed-loop flux observer for sensor less torque control of standard induction machines", Proceedings of PESC 95 - Power Electronics Specialist Conference PESC-95, 1995.

[35] Ming Meng. "Voltage Vector Controller for Rotor Field-Oriented Control of Induction Motor Based on Motional Electromotive Force" , 2007 2nd IEEE Conference on Industrial Electronics and Applications, 05/2007.

[36] Yinhai, Zhang, and Chen Zhikui. "An Asynchronous Motor Vector Control System Considering the Variation of Rotor Resistance", 2012 Third International Conference on Networking and Distributed Computing, 2012.

[37] Choudhury, Abhijit, and Kishore Chatterjee. "Modified stator flux estimation-based direct torque controlled induction motor drive with constant switching frequency operation"International Journal of Power Electronics, 2012.

[38] L.Q. Zhou. "Direct Torque Control of Synchronous Reluctance Machine Based on Modified Integrator" , 2007 Power Conversion Conference - Nagoya, 04/2007.

[39] A.H.M. Yatim. "An improved stator flux estimation in steady state operation for direct torque control of induction machines" , Conference Record of the 2000 IEEE Industry Applications Conference Thirty-fifth IAS Annual Meeting and World Conference on Industrial Applications of Electrical Energy (Cat No 00CH37129) IAS-00, 2000.

[40] N.R.N. Idris. "An improved stator flux estimation in steady-state operation for direct torque control of induction machines" , IEEE Transactions on Industry Applications, 2002.

[41] Roberto Menis. "A Direct Torque Control Scheme for Induction Motor Drives Using the Current Model Flux Estimation" , 2007 IEEE International Symposium on Diagnostics for Electric Machines Power Electronics and Drives, 09/2007.

[42] M. Pastorelli. "Direct torque control of induction machines over a wide speed range" Conference Record of the 1992 IEEE Industry Applications Society Annual Meeting, 1992.

[43] Menaa, M.. "Sensorless direct vector control ofan induction motor" , Control Engineering Practice, 2008.

[44] Venugopal, Chitra. "Fuzzy logic based DTC for speed control of Matrix Converter fed Induction Motor" , 2010 IEEE International Conference on Power and Energy, 2010

[45] R. Krishnan, "Vector Control of Induction Motor Drives" in Electric Motor Drives modeling, analysis and control, 2nd ed, New Jersey, prentice hall ,2001, ch.8, pp. 411-513

[46] Bimal.K.Bose, "Control and Estimation of Induction Motor Drives" in Modern Power Electronics and AC Drives, 2002,ch.8, pp.333-439

[47] Jose Rodriguez and Patricio Cortes, "Model Predictive Control" in Predictive Control Of Power Converters And Electrical Drives,1st ed,Wiley,20012, ch.3, pp 31-38.

[48] Jose Rodriguez and Patricio Cortes, "Predictive Control of a Three-Phase Inverter" in Predictive Control Of Power Converters And Electrical Drives,1st ed,Wiley,20012, ch.4, pp 43-63.

[49] Kumar, M. Dilip, S. F Kodad, and B. Sarvesh."Detection of fault in VSI of Vector controlled induction motor drive system" , 2015 Conference on Power Control Communication and Computational Technologies for Sustainable Growth (PCCCTSG), 2015